Regeneratable Magnetic Iron Oxide Embedded Chitosan Beads For Optimized Adsorption Treatment of Nitrate Containing Mine Water

By

Muntaha Nasir

School of Chemical and Materials Engineering

National University of Sciences and Technology

2022

Regeneratable Magnetic Iron Oxide Embedded Chitosan Beads For Optimized Adsorption Treatment of Nitrate Containing Mine Water

Name: Muntaha Nasir

Reg. Number: 00000335831

This thesis is submitted as a partial fulfillment of the requirements for the degree of

MS in Nanoscience and Engineering (MS NSE)

Supervisor: Prof. Dr. Nasir M. Ahmed

School of Chemical and Materials Engineering (SCME)

National University of Sciences and Technology (NUST)

H-12 Islamabad, Pakistan

November, 2022

Dedication

I would like to devote my

thesis

to my beloved family and my research administrators

Acknowledgement

All praise belongs to the All-Powerful Allah (SWT), whose magnificence is indescribable in words. His blessings are immeasurable. I am grateful to my creator for giving me the opportunity to gain experience during this study, and for giving me the stamina to do this research. I was given guidance in my research by my supervisor, Prof. Dr. Nasir M. Ahmed. Working under the direction of Prof. Dr. Nasir M. Ahmed was a privilege and an honor for me. I owe a great deal of gratitude to the members of my GEC for their help and support in completing my work. My words cannot express how grateful I am to my parents, siblings, and husband; their support, love, and prayers have made a significant difference in my life. The moral support of my friends Ayesha, Summayya and Uswa were always there for me.

Muntaha Nasir

Abstract

Industries and their sites across the world are a major contributor to pollution in water, among which Nitrates possess the most toxic effects. To overcome this problem a productive method is needed for the removal of Nitrate from water. Therefore, chitosan beads, a non-toxic, biocompatible and biodegradable polymer, have showed great potential in numerous applications, including the removal of different salt ions and heavy metals from water. In this study Nano scale Iron Oxide particles produced by Co-precipitation method were embedded in chitosan by using chemical co-precipitation method, resulting in beads. The performance of Iron Oxide embedded chitosan beads (IECB) in a batch system has been studied, for nitrate adsorption from industrial water. Concentration of nitrate in solution was determined via UV Vis spectrophotometry. Physiochemical properties of IECB were characterized through XRD, SEM, FTIR, VSM, contact angle and BET. Multiple factors influencing the adsorption attitude of IECB such as adsorbent dosage, initial concentration, pH and the interaction time of Nitrate ions were measured: pH=5, 24 °C in 2 hrs. In this study, the Langmuir isotherm model (R^2 > 0.991) and pseudo second order kinetics (R^2 > 0.984) best fitted the experimental. Regeneration experiment was performed up to 5^{th} cycle in which efficiency was dropped from 93% to 79%.

Table of Contents

List of Figures

List of Tables

Abbreviations

NO_3^-	Nitrate
Ce	Equilibrium conc. (mg/l)
Co	Initial conc. (mg/l)
Kl	Langmuir constant
Kf	Freundlich constant
n	Freundlich exponent
q_e	Equilibrium adsorption (mg/g)
Q_t (mg/g)	Adsorbed amount at time "t"
$k1$ (l/min)	Pseudo-first order rate constant
e	Exponential function
Fe_2O_3	Ferric oxide
OH,	hydroxyl group
NaOH	Sodium Hydroxide
$FeCl_3.6H_2O$	Iron (III) Chloride Hexahydrate
$(C_2H_2OH)_2$	Ethylene Glycol
$(FeCl_2.4H_2O)$	Iron (II) Chloride Tetrahydrate
$(C_6H_{11}NO_4)$ n	Chitosan
PVP	Polyvinylpyrrolidone

Chapter: 1

Introduction

1.1 Background:

1.1.1 Environmental Pollution

Environmental pollution is defined as the contamination of the earth and atmospheric system's biological and physical constituents such that normal environmental processes are gravely impacted. [1]

Despite it not being a new phenomenon, pollution is still considered the most significant threat to humanity and the primary cause of environmental mortality and disease. Industrialization, exploration, mining and urbanization have had the most substantial impact on global pollution. [2] Richer countries' beliefs and stricter laws are doing much to protect the environment but developed and developing countries share the burden. Despite increasing attention, pollution remains a problem. [3]

Pollutants may induce primary or secondary damage, the primary damages to be quantified and have substantial impacts.[2] On the other hand, the secondary harm appears as a slight disruption to the delicately balanced biological food chain pyramid and is only detectable over extended periods. [4]

These undesirable consequences could have an immediate human impact or might be moderated by resource species or even climate change. Different classes of pollution vary based on the pollutant types used and any later pollution or environmental factors.

1. Water pollution
2. Soil/land pollution
3. Air pollution
4. Noise pollution
5. Thermal pollution
6. Radioactive pollution

Air pollution causes the most damage to the environment, people, plants, animals, and all other living creatures among these several kinds of pollution.

1.2 Water Pollution

Water contamination comes about because of pollutants contaminating water sources thus making the water unsuitable for activities including but not limited to drinking, cooking, swimming and washing. Lakes and oceans can be contaminated by air pollution. Moreover, land contamination could also lead to underground streams, rivers and the ocean becoming contaminated. Thus, trash discarded in empty lots could eventually lead to a water source becoming contaminated.

Pollutants in water can poison people or even cause the spread of disease. Badly treated sewage may have bacteria and parasites that can get into drinking water supplies and cause illnesses like cholera and diarrhea.[5] Harmful materials such as pesticides, herbicides, and chemicals from farms, residences, golf courses and business can be fatal and some may cause chronic toxic effects leading to cancer or even neurological issues. By using fresh water for preparing food or for consumption, we allow the entrance of water contaminants into our bodies. After the digestive system encounters contaminants, they then spread to other organs in the body and cause diseases. Skin irritations are a common occurrence arising from coming into contact with chemicals while swimming in contaminated water or washing clothes. Waterways often carry hazardous substances that could affect local plant and animal life. While most organisms would try to survive by keeping the toxic contaminants in their bodies, humans would consume them and end up unwell or diseased. Some flora and fauna may also die due to excessive contamination or have their essential functions severely impacted. It is possible for plants and animals to perish or not reproduce properly.[6]

Water quality guidelines come in a variety of forms. Stream standards set up permitted quantities of chemicals or attributes (such as dissolved oxygen, turbidity, or pH) allowed in those water bodies, based on their given categorization.[7] They classify rivers, streams, and lakes based on their greatest beneficial use. The quantities of pollutants (such as biological oxygen demand, suspended particles, and nitrogen) that are allowed in the final discharge from treated wastewater are regulated by effluent (water outflow) standards.[8] The quantities of specific contaminants that are allowed

in drinking water that is distributed to households for domestic consumption are regulated by drinking-water standards.[9]

1.3 Industrial Wastewater

Water pollution is primarily caused by industrial waste. Manufacturing operations in business units, industrial duties, mill trash, and extracting operational matters are only a few examples of industrial processes that result in the production of trash, which is made up of any worthless and dangerous materials.[2]

The variety of trash generated by corporations includes dust, shingles, brick walls, hard surfaces, waste metals, oil particulates, alchemical materials, chemical compounds, organic and inorganic compounds, salts, and even food waste, particularly from cafeterias.[5] Heavy metal ions from mill waste such as mercury (Hg), cadmium (Cd), and arsenic are also present which has high solubility in water.[10]

1.4 Mine Water

Water that accumulated in a mine and must be transported to the surface using water management techniques for the mine to continue operating is known as mine water or mining water.[11]

The miner makes a distinction between groundwater and surface waters even though all the water entering pit workings is the result of atmospheric precipitation. Surface water enters the pit through holes in the mine just at the surface of the ground, including underground structures or shaft entrances.[12] Heavy rains cause water to seep into the ground, where it meets levels of impervious rock to generate groundwater. Pit water mostly consists of seeping groundwater and interstitial water into the mines.[9]

Tailings (the leftover material after the valuable ore is sorted out) and overburden are my principal products of the mine.[13] Treating the mining water before it is released into the surrounding environment is a big problem because the water inside and surrounding the mine is typically contaminated throughout the mining procedure. Mineable grades for various ores range from a few ppm to an order of a

percent. This shows that most of the materials disturbed during mining are garbage since 99 tons of waste are typically produced for every ton of copper metal extracted.

1.4.1 Mine Water Characteristics

Until mine water is contaminated, it is generally identical to groundwater. The aquifers' bedrock and water conservation levels determine their water quality features. The pH of mine water varies from essentially neutral to only just alkaline. A hazardous concentration of mine water is usually under the detection limit if the mineral is modest. As part of the mining process, the mine water is altered by passing it through the mining operations and road. The water is combined with rock powders, coal granules, and other organic materials. If the water is contaminated, it will be greyish black in color, have a lot of suspended particles, and have some microbes in it.[13]

There are several ways to combine mine water during production, with mining and ore processing water making up most of it. The following are the primary sources of mine wastewater:

1. Wastewater from open-pit mines is created throughout the mining process; acidic water is released from waste rock piles after the waste rock piles dissolve after rain.[14]

2. Mine wastewater is primarily production-related groundwater contamination.

3. Wastewater created during the washing, crushing, and mineral processing processes are referred to as "mineral processing wastewater." Significantly polluted wastewater often has ore, metal flakes, or other mineral processing chemicals. The dam accumulated wastewater.[15]

4. Domestic wastewater, hospital wastewater, and wastewater from car washing all have solid suspended particles, petroleum, organic compounds, and other contaminants.[16]

1.4.2 Mine Wastewater Classification

Clean and divert, sewage and divert, classify, and treat, and quality and reuse are the general guiding concepts of sewage treatment and reuse. Dewatering water, water in the goaf, and underground sewage in the mine make up the three primary categories of mine drainage.

1. Draining water: draining water in mines refers to the wastewater that is generated underground due to the formation structure in the mining

2. Mine underground sewage: During mining operations, aquifers having coal will naturally be drained, and the resulting waters will mix to generate mine water at the well's bottom. The primary contamination features of mine water vary depending on the type of mine and are typically categorized as clean groundwater, suspending mine water, acid mine water including acid pollution, highly saline mine water, and special polluted mine water.[17]
3. Clean mine water: It has good quality, a pH that is often neutral, low turbidity, a low degree of hardness, and is free of hazardous ions. This mining water can be caught at the water source, released down the pipeline to the well's bottom, and then carried to the surface by the pumps. After quick disinfection, this sort of water could be used for drinking, and water having healthy elements can be used as mineral water. [7]
4. Acid mine water: Wastewater with a pH less than 6 is typically referred to as acid mine water. It develops when groundwater seeps through the mine's bottom layer and is oxidized by bacteria and sufficient oxygen to produce sulfurous acid and sulfuric acid, leaving the mine water very acidic. [18]
5. Having specific polluted mine water: Fluoride, heavy metals, and radioactive components are only a few harmful compounds that can be found in mine water that has unique pollutants added to them. This mine water is seriously polluted and difficult to manage.[19] The ecological environment will suffer from random discharge, which will also have an impact on how mine water resources are used.

1.5 Effect of Toxicity from Industrial Wastewater

The number of contaminants in the environment has increased because of recent rapid industrialization. All types of biological forms have been negatively affected, either directly or indirectly, by the improper management of some dangerous industrial wastes that were disposed of into bodies of water. Heavy metals are just one among many types of water pollutants that are persistent and not biodegradable. The ingestion of specific harmful heavy metals as part of a food chain could negatively affect other creatures and humans.[19] They may be teratogenic and carcinogenic, damaging organs, disrupting the nervous system, creating oxidative stress, and hindering growth and development. Another commonly occurring type of chemical pollution that is produced from industrial processes is phenolic compounds. They impede microbial

function which can in turn cause interference with any biological therapeutic procedures. In addition, they have the power to lead to reflex loss, perspiration, lower body temperature, cyanosis, reduced breathing, and respiratory failure. The main components of the pulp and paper industry's effluent, such as tannins, resins, and chlorinated organic compounds, can be mutagenic and genotoxic.[13] Organic material and its derivatives are the most typical effluent form of the paper pulp sector. Due to their poor biodegradability and potential for transformation into hazardous chemicals during biological processing, they may impair aquatic species' hormonal balance.[20] The microbiological activity of non-salt-adapted microorganisms is significantly affected by the hyper salinity of water, and it can also obstruct aerobic treatment procedures. Toxic contaminants must therefore be effectively removed before being released into different water bodies if we want to keep a clean and healthy ecosystem.

1.6 Sources of Nitrates Contamination

The main sources of nitrate in groundwater are fertilizers, septic tanks, and manure storage or application processes. Nitrogen from fertilizer that is not absorbed by the plants, volatilized, or removed by surface runoff eventually ends up as nitrate in the water.[21] As a result, the nitrogen becomes inaccessible to the plants and the concentration in the groundwater may rise above the acceptable limits for safe drinking water.[22] Fields, barnyards, and storage areas can all similarly lose manure’s nitrogen. Groundwater nitrate concentrations rise because of septic systems' inability to fully remove all the nitrogen present in wastewater.[23]

Table 1: Sources of nitrate contamination in diverse ways

	AGRICULTURE	MUNICIPAL	INDUSTRIAL
DIFFUSE SOURCES	-Use of synthetic nitrogen-based fertilizers. -Use of organic fertilizers.	-Combustion engines from vehicles. -Disposal of municipal effluents by sludge spreading on fields.	-Atmospheric emissions from energy production. -Emission from combustion engines. -Industrial effluents disposal.
LINEAR AND POINT SOURCES	-Accidental spills of nitrogen-rich compounds. -Absence of slurry storage facilities. -Leaking Slurry or manure tanks.	-Old and badly designed landfills. -Septic tanks. -Leaking sewerage Systems.	- Nitrogen-rich wastes disposal via various well injection techniques.

Table 2: Additional sources of nitrate contamination

Other Sources of Nitrates	-Animals Waste. -Domestic sewage. -Shallow, rural domestic wells. - Poorly constructed wells that mix up the polluted layer with the non-polluted aquifer layer.

1.7 Effects of Nitrates Contamination

Nitrate pollution is currently one of the main issues facing groundwater management. A molecule that results from the oxidation of nitrogen is called a nitrate. It exists both naturally and synthetically, and if it is not controlled, it can have profoundly serious, detrimental impacts on both living things and the environment.[21]

Nitrates are a serious hazard to freshwater creatures including invertebrates, fish, and amphibians because they can change pigments that carry oxygen into pigments that can no longer transport oxygen.[24] Freshwater creatures are particularly vulnerable to contaminants, hence as nitrate concentrations rise, so does the level of nitrate toxicity towards aquatic life. Long-term exposure to excessive nitrate levels can result in the extinction of some species and the destruction of entire ecosystems.[25]

Nitrate concentrations not only endanger human health but also aquatic life's ability to survive.[23] Humans are not evolved to eat these high quantities, which are often ingested through drinking water, and consuming excessive amounts can have serious negative health effects.

Cancer, thyroid illness, and other acute problems may result from nitrate water contamination. Overall, it is abundantly obvious that nitrate poisoning has negative consequences on humans, aquatic life, and the ecosystem.[26]

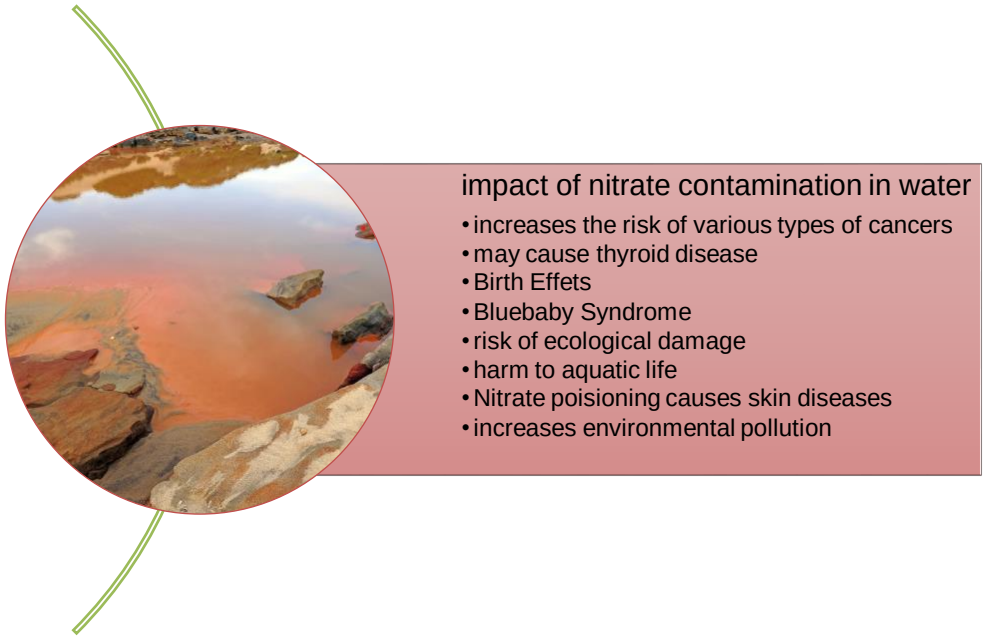

Figure 1: Impact of nitrate contamination in water

1.8 Adsorption Processes

The adsorption process is the binding of ions, atoms, or molecules from solid, liquid, or gas to a solid surface. Adsorption is the term used to describe the collection of ions, atoms, or molecules by the solid's internal or external surface. In this situation, the solid surfaces employed to adsorb dissolved substances or gases are known as adsorbents, and the total amount of adsorbed mass is referred to as adsorbate. In the adsorption separation process, the material is taken out of a fluid by being transferred to a solid phase.[27]

Like surface tension, adsorption is regarded because of surface energy. Atoms are joined to one another in bulk materials through a variety of bonding, including ionic, covalent, coordinate covalent, h - bonding, and metallic bonding.[28] Adsorbents may easily form bonds with adsorbates because, on the interface of absorbent, all atoms and molecules are not completely linked with the other different atoms.

1.8.1 Adsorption Mechanism

Adsorption can be conducted in a single step or over the course of several processes. While nitrate is adsorbed onto the surface of the adsorbent in three steps

i. Nitrate particles migrated towards the surface of the adsorbent
ii. The complexed aqueous Nitrate separation
iii. Diffusion on the surface of the substrate.

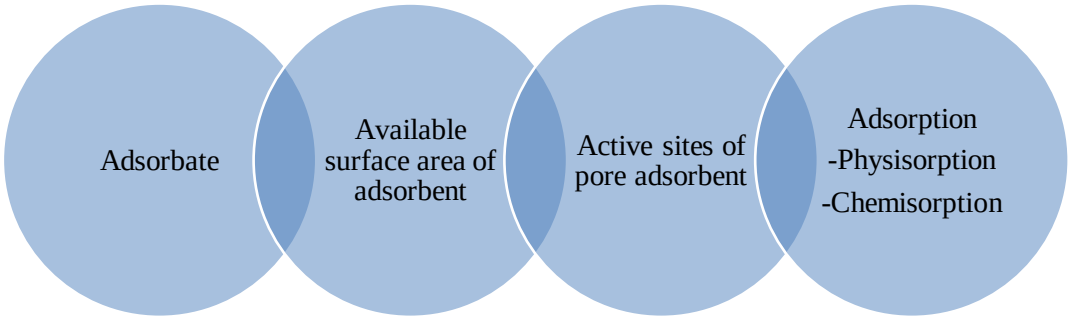

Figure 2: Adsorption mechanism

The materials to be adsorbed first spread on the outer surface of the adsorbent because of intermolecular interactions between the adsorbent and adsorbate.[27] Adsorbate atoms moved into the pores of the surface of the adsorbent in the second step because the adsorbent surface had many pores. In the last step, these adsorbate atoms will fill the pore volume and then produce a layer of approached atoms, groups of approached atoms, and atoms to the adsorbent's sites of action.

1.9 Adsorption Isotherms

The equilibrium relation between the adsorbate adsorbed upon that surface of an adsorbent at constant temperature and the sorbent adsorbed in the liquid phase is known as the adsorption isotherm.[29] To assess the mechanism and effectiveness of the adsorption process, it is important to study the specifics of kinetics (pace of sorption) and thermodynamics (interfacial energy at final equilibrium). The solute absorption rate finds the length of time needed to complete the reaction and achieve the flow through the system or any fixed bed by studying the adsorption kinetics.

1.9.1 Langmuir Isotherm

This model is based on some assumptions

- Adsorption of molecule on the surface of the adsorbent is chemisorption.
- Single layer adsorption occurs and localized
- Molecules accommodated active sites
- Homogeneous Surface

Langmuir's isotherm model will only be useful in the condition of homogeneous adsorption. Whereas to uniformly adsorb on the outside, all adsorbate atoms, ions, and molecules needed to have the same sorption activation energy. It is primarily employed in the adsorption process from liquid solutions.[30] In mathematics, a linear equation is depicted that can be written as:

$$\frac{Ce}{qm} + \frac{Kl}{qm} = \frac{Ce}{qe}$$

- "Ce" is the concentration of adsorbent at equilibrium (mg/l)
- "Kl" is the constant of Langmuir
- "qm" maximum amount of adsorbent for monolayer (mg/g)

According to the Langmuir isotherm model of chemically adsorbed metal ions, each active site should only grasp one adsorbate.[29]

1.9.2 Freundlich Isotherm

This model shows non-ideal adsorption and suitable for

- Heterogenous surfaces
- Multi-layered adsorption
- Distribution of energy with affinity overactive sites

Freundlich adsorption isotherm model is for complex adsorption and heterogeneous surfaces, it is noted that its linear form is written as follows,

$$\text{Log Qe} = \log \text{Kf} + 1/\text{n} \log \text{Ce}$$

- "Kf" is the Freundlich's constant
- "n" is the Freundlich's exponent

1.10 Adsorption Kinetics

The concentration of the reactant, which is predicted by the reactant's kinetic equations, which are determined experimentally using compiled data from the experiment, finds the rate of reaction. Vital details and the mechanics of Adsorption kinetics can be used to obtain the reaction.[31] Adsorbate and adsorbent chemical and physical qualities have a significant impact on the kinetics of adsorption, which in turn affects the mechanism of adsorption. Kinetics investigates how the adsorption process is affected by time and initial concentration. Unlike under experimental conditions for the process of adsorption, many kinetics models have been studying the adsorption mechanism.[32] The overall assessment by using pseudo-first order and pseudo-second-order processes, the mechanism of adsorption is determined.

1.10.1 Pseudo-First Order Kinetics

The liquid and solid adsorption systems are primarily defined by the Laguerre Pseudo-first order kinetics of adsorption.[33] The equation is the basis for this concept is mathematically written as

$$\ln (qe - qt) = \ln qe - k1\text{t}$$

- "qe" is absorbent adsorbed at equilibrium (mg/g)
- "qt" is adsorbent adsorbed at a time 't' (mg/g)
- "$k1$" is the rate constant of pseudo-first order (l/min)

1.10.2 Pseudo-Second Order Kinetics

The pseudo-second-order model could be completely employed to show the adsorption kinetics.[34] The mathematical form of it is as follows:

$$\frac{1}{k_2 qe^2} + \frac{t}{qe} = \frac{t}{qt}$$

- "qe" is the adsorbed amount at equilibrium (mg/g)
- "qt" is the absorbed amount at a time 't' (mg/g)
- "$k2$" is pseudo second rate constant order (g/ (mg. min)

1.11 Aims and Objectives

- Synthesizing the magnetic chitosan beads.
- Studying the effect of pH, concentration, contact time, and effect of adsorbent dosage by batch adsorption process.
- Applying adsorption isotherm and adsorption kinetic models to the results of batch testing.
- Determining the efficient removal percentage of nitrate from water.
- Regeneration of these beads up to multiple cycles i.e., reusing these beads.

Chapter: 2

Literature Review

2.1 Nitrate Removal Technologies

Diverse technologies and methods are being created and used to remove contaminants from wastewater produced from many sectors from which one of the major pollutants is Nitrate.[35] The removal of nitrates from the water is very necessary as it is one of the most dangerous types of contaminants.

Nitrate removal methods are classified into two categories, either physical-chemical removal methods or biological removal technique.

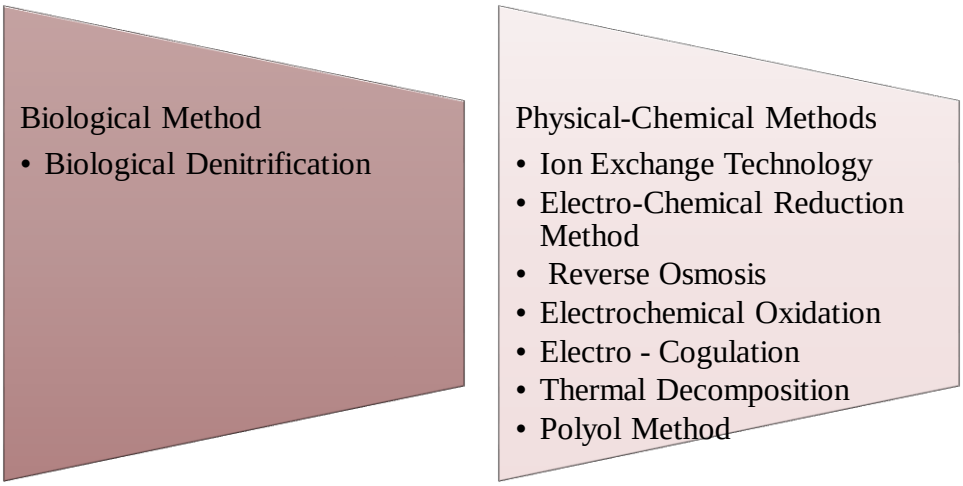

Figure 3: Nitrate removal technologies

2.1.1 Biological Denitrification

After nitrification, a bacterial-based process, comes biological denitrification. It is the last phase of the nitrogen cycle, a biological process that naturally converts nitroform by one form to the other. The biological treatment of wastewater depends on both nitrification and denitrification.[36] As a result of soil nitrates or nitrites being chemically reduced, denitrifying bacteria cause the loss of gaseous nitrogen. Some microorganisms use nitrate to promote respiration when oxygen is scarce.[1]

For the following reasons, substantial research on denitrification has been done during the past century. First off, denitrification is a key part of the biological nitrogen cycle, which keeps the equilibrium of the world's nitrogen budget by returning reactive

nitrogen to the atmosphere.[10] Secondly, denitrification has indeed been widely used in engineered treating wastewater for targeting water quality improvement as one of the important steps to achieve biological nitrogen removal (BNR). Third, microbial denitrification can increase the amount of nitrous oxide (N2O) released into the atmosphere, which is about 300 times more powerful than carbon.[37]

Activated sludge technology outpaces biofilm processes. The same amount of recirculation and alternate procedures are employed. 4–10 mg/l of inorganic nitrogen is the normal effluent purity that can be reached over the long term on average. It is possible to obtain effluent concentrations of 2-3 mg N/l in some situations. The main elements in wastewater are nitrate and soluble organic nitrogen.[38] The dissolved organic nitrogen level of these two is challenging to regulate.[23]

The advantages of Biological Denitrification are as follows:

- High nitrate removal efficiency.
- Cost-friendly process
- Good stability of the process
- Reliable process
- The process can be controlled with ease

2.1.2 Ion Exchange Technology

The elimination of nitrates through ion exchange is a quick and efficient method. It works in an analogous way to a typical filtration system and can easily get rid of well over 90% of the nitrates. [39] Common salt (NaCl) or potassium chloride (KCl) is used in the process to regenerate a strong-base anion exchange resin. The resin uses the salt's chloride ion for its purposes. The sodium ion does not impede the process; it just flows through the resin bed. Nitrate removal has long been carried out using ion exchange resins. "Nitrate-selective" and "standard" are the two types that are typically available. The relative affinity of multivalent ions such as sulphate and ammonium sulphate are the main distinction between them.[30]

Standard Types 1 and 2 resins have the following relative affinities, in decreasing order of stronger affinity: perchlorate >> sulphate >> arsenate >> nitrate >> chloride >> bicarbonate.

In contrast, multivalent ions like sulphate & arsenate are de-selective for nitrate-selective resins. In comparison to all the common ions found in water, including sulphates, these resins have a higher affinity for nitrates. The following ions have a higher affinity for nitrate-selective resins than others: perchlorate, nitrate, sulphate, arsenate, chloride, and bicarbonate.[25]

Pre-treatment for nitrate removal systems typically just includes pre-filtration and de-chlorination (when chlorine is present). These two procedures are needed to prevent physical fouling and oxidation from damaging the anion bed.[40] Except in circumstances of high pH and high hard water (4 grains or higher), when the amount of calcium carbonate and hydroxide ions in the resin bed could produce a precipitate of calcium or magnesium, softening before the nitrate removal resins is not necessary.[39, 41] If this occurs, it might be necessary to briefly soak or rinse the resin bed in a moderate acid.[42]

Based on the various kinds of bacteria, the relative affinities of nitrates over sulphates in nitrate-selective resins are typically 10 to 100 times higher than those in ordinary resins.[30] As a result, the sulphate ion would be "dumped."

The treated water's nitrate concentration progressively increases to its inflow concentration when a nitrate-selective resin is operated past the point of exhaustion.[43] The effluent's sulphate concentration will surpass that of the input concentration.

Depending on the application, there are various nitrate-selective resin varieties, each with unique benefits.[44] Due to its smaller size than the tributylamine type, the triethylamine structure produces a resin with a better working ability.[45] However, when regenerant use is reduced through brine reclamation plans, the tributylamine may offer lower chemical running costs in big systems.[41]

2.1.3 Electrochemical Reduction Method

The electro-reduction technique of therapy has several benefits, including the need for no chemicals, a limited area, and cheap investment cost. In situations when the biological technique cannot be used, electrochemical methods are proper for extracting nitrate ions from strong aqueous solutions that result through reverse osmosis, ion filters, and wastes that have been neutralized with nitric acid.[41] For many years,

researchers have been studying the electrochemical reduction of nitrate using copper and various modifications of the copper electrodes.[46]

Most of these studies were conducted under various circumstances, making it challenging to directly compare the results. Nevertheless, it has been demonstrated that copper reacts to nitrate reduction the most quickly. Some electrodes, including Cu and Fe, are recognized as effective promoters for electrochemical nitrate reduction.[47] However, electrochemical reduction of nitrates results in a very wide range of compounds, including N2, NH2OH, N2O, and NH3, as reduction of NO3- ions is one of a range of methods for its removal from wastewater.

Regarding the electrochemical reduction of nitrate on different metallic electrodes, many efforts have been performed up to this point. Since nitrate is one of the eight potential products, along with NO2, NO2, NO, N2O, N2, NH2OH, NH3, and NH2NH2, it has been proved that it is difficult to convert nitrate into harmless nitrogen gas.[48] The primary by-products of an acid electrolyte have also been found to be hydroxylamine and hydrazine when the accompanying electrolytes are basic or neutral.[49]

The cathodic reaction of electrochemical reduction process are as follows:

$NO_3^- + H_2O + 2e \leftrightarrow NO_2^- + 2OH$

$NO_3^- + 3H_2O + 5e \leftrightarrow 12N_2 + 6OH^-$

$NO_3^- + 6H_2O + 8e \leftrightarrow NH_3 + 9OH^-$

$NO_2^- + 2H_2O + 3e \leftrightarrow 12N_2 + 4OH^-$

$NO_2^- + 5H_2O + 6e \leftrightarrow NH_3 + 7OH^-$

$NO_2^- + 4H_2O + 4e \leftrightarrow NH_2OH + 5OH^-$

The main side reaction at cathode is hydrogen evolution

$2H_2O + 2e \leftrightarrow H_2 + 2OH^-$

At anode there is oxygen evolution

$$4OH^- \leftrightarrow O_2 + 2H_2O + 2OH^-$$

Overall reaction is

$$NaNO_3 + 2H_2O \leftrightarrow 2N_2 + 5O_2 + 4NaOH$$

2.1.4 Electro-Chemical Oxidation Method

It is the type of chemical reaction in which the oxidation state of the substrate changes. There are several types of oxidation processes for the removal of nitrate and water purification.[46] Two alternative oxidation mechanisms—direct oxide layer oxidation, in which the pollutants were destroyed there at the anode surface, and indirect oxidation, where a mediator—HClO, H2S2O8, and others—is electrochemically produced to carry out the oxidation—can be used to electrochemically oxidize pollutants.[50] it is possible for both mechanisms of oxidation to coexist while the electro-oxidation of any aqueous effluents occurs.

In Direct Oxidation, pollutants are directly oxidized in two steps:

(1) they are diffused from the bulk solution to the anode surface

(2) they are oxidized at the anode surface.

As a result, the relationship between substrate mass transfer and electron transport at the electrode surface will determine how effective the electrochemical process is.[51] The electrode activity and current density control the rate of electron transport.

There are two routes that organic contaminants can take during anodic oxidation:

- Conversion using electrochemistry. Only a small portion of organic substances are oxidized. Consequently, a follow-up treatment may be necessary.

$$R \rightarrow RO + e^-$$

- Electrochemical Combustion, Burning electrochemically. Water, carbon dioxide, and other inorganic substances are produced from organic compounds:

$$R \rightarrow CO_2 + H_2O + salts + e^-$$

Indirect electrochemical oxidation involves the electro-generation of a potent oxidizing agent at the anode surface, which then obliterates the contaminants in the bulk solution.[41] Chlorine, which is created when chloride is oxidized at the anode, is the most prevalent electrochemical oxidant. Ammonia oxidation is typically considered to occur by this pathway, even though the involvement of active chlorine in the oxidization of organic contaminants is unclear.[48] The widespread occurrence of chloride in wastewater waters and it is very efficient action is to blame for the large usage of active chlorine. In addition to oxygen, peroxide, peroxodisulfuric acid (HS2O8), and ozone can all be created electrochemically. [47]

2.1.5 Electrocoagulation

Electrocoagulation is a cutting-edge and affordable water treatment method that is been shown to be successful in removing suspended particulates, dissolving emulsifiers, and depolluting heavy metals.[52] The first-time electrocoagulation was used in wastewater treatment to produce coagulation on-site was in 1889. Recent years have seen a resurgence in interest in electrocoagulation (EC) technology because of the need for alternate wastewater treatment methods.[53] EC can be defined as the in-situ production of coagulants through electrochemical reactions involving a "sacrificial" anode that result in the anode's dissociation in the effluent wastewater.[54] Metal ions that destabilize, agglomerate, and condense dissolved pollutants can produce large-scale coagulated metal hydroxides. The lack of chemical addition, lower capital expenditures, decreased sludge production, and low power requirements are only a few of the many benefits of EC. The high conductivity of wastewater and the need to update the electrodes are two drawbacks of the EC, nevertheless.[55]

A reference electrode is used to treat water in the electrocoagulation process. A DC or AC power supply with a microcontroller and a current is used to connect the two electrodes, the cathode, and the anode, which is submerged in the electrolytes or a conducting solution, to form an electrochemical cell.[56] During the electrolysis process, oxidation and reduction reactions take place by passing an electrical current through the electrolytic solution. Mineral ions that function as coagulation ions in situ in aqueous are produced by the sacrificial anode. These ions are produced because of an anode dissolving.

Because they are readily available, affordable, and non-toxic, the electrodes are typically made of iron, aluminum, and stainless steel. It so becomes the primary electrode material used in the EC technique. In an EC system, the placement of electrocoagulation systems varies; the electrodes may be either one or there are more anode-cathode pairs, and they are connected in either monopoles or bipolar.[55] Metallic cations produced by the anode hydrolyze to produce polyhydroxides, hydroxides and polyhydroxy Together with strong convergence for anti-ions and scattered particles, mineral compounds produce coagulation. Because the likelihood of an electric twin layer's being out of harmony has decreased, they will lower the surface net total of colloid particles that are suspended.[57]

When particles are close enough to one another to cause particle agglomeration because of the repulsion of the suspended particles, van der Waals force takes precedence.[53] When salts are used in water treatment facilities for chemical coagulation, the two phases of flocculation and coagulation are distinguished based on how long each process takes or are physically isolated from one another. The coagulation and flocculation processes occur simultaneously during electrocoagulation, making it impossible to distinguish between the two phases.[58]

2.1.6 Reverse Osmosis

A contemporary approach to wastewater treatment is reverse osmosis. Without the addition of chemicals, resins, or ion exchange beds, the forefront spiral design of membranes removes the pollutants from the water feed.[59] It is possible for manufacturing wastewater to have harmful by-products.

When it comes to handling and treating wastewater, particularly in industrial operations, reverse osmosis (RO) is becoming increasingly common.[60] Businesses are becoming more conscious of how significant a responsibility handling such vast amounts of water is. Companies ought to invest in water purification technologies like RO.[61] They offer a safer work environment, require less upkeep, and eventually result in cost savings. Additionally, they must adhere to specific rules and laws.[62]

While there are several water filtering options for managing and treating wastewater, RO is growing in popularity. RO has a 99.9% rejection rate for germs.[42]

Systems for reverse osmosis can be used in conjunction with other water purification devices.[63] The type of water you need to treat and the type of water you want to

reuse depend on each water solution. As raw quality of water varies depending on location, this will be different for each solution.[64] The usage of pollutants during production also affects the outcome. RO purges contaminants from tainted water to function.[61] By applying pressure and driving the polluted solution through membranes, it accomplishes this. After being treated, the water can either be securely disposed of or used again in production. below is the Schematic for reverse osmosis [65]

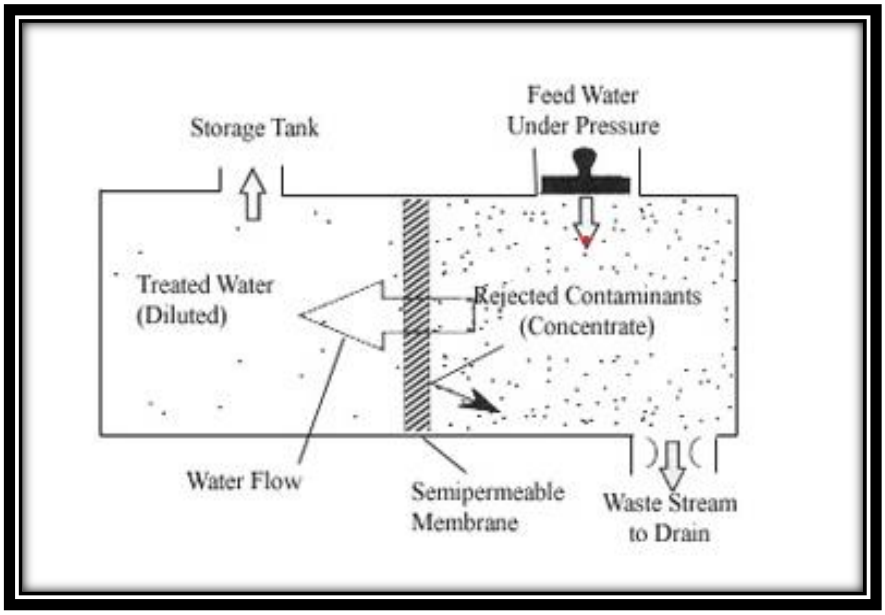

Figure 4: Schematic for reverse osmosis

2.2 Synthesis of Iron Oxide Nanoparticles

Iron and oxygen are the two most prevalent elements found in nature. Iron oxide nanoparticles have been produced using a variety of methods, and the final product has a mixture of divergent phases.[45] In general, organic processes like co-precipitation and hydrothermal synthesis can be used to change the characteristics of iron oxide particles. However, it is not possible to make iron oxide nanoparticles on a large scale quickly without using intermittent and batch processes. The essential nanoparticles with the right hypnotic qualities, size, and shape can be created using a variety of chemical, non-living, and pathobiological approaches.[66]

Iron typically exists in two different oxidation states in iron oxide, namely Fe-2 with four unpaired electrons in the third shell as well as five unpaired electrons in the third subshell of Fe+3. Due to its importance as a transition metal and as a necessary magnetic material for technology, iron oxide has received much research. It is made of magnetite, which has a face-centered cubic (FCC) and spinal crystal structure. It is

black in color.[32] Rhombi-dodecahedron and octahedron are the two types of crystals found in magnetite iron oxide, and their surface areas range from 4 to 100 (m2/g). Compared to other metallic nanomaterials, the magnetic iron oxide material is more effective in terms of chemical stability and biocompatibility.[67]

In nature, Fe3O4 is found as the inert magnetite. It is made up of iron (II) and iron (III) ions as well as iron oxide on occasion. Fe2O3 Iron oxide is sometimes known as black powder. Since it typically exhibits persistent magnetism, it is referred to as ferromagnetic substance in nature. The only use for Fe3O4 on a wide scale is as a black pigment powder, which is why it has been produced in the lab rather than extracted from naturally occurring minerals.[68] While we can alter its shape and particle size depending on our needs by modifying the synthesis procedure.

The octahedral centers of Fe3O4's counter spinel cubic system, which consists of uniformly dispersed Fe3+ ions over the remaining octahedral spaces and the tetrahedral spots and firmly linked cubic lines of oxide ions and whole Fe2+ ions, are located at their centers.[69] Additionally, like Fe3O4, alike FeO and Fe2O3 have a close-packed cubic structure. Fe3O4 has a significantly better electrical conductivity than Fe2O3.

2.2.1 Multiple Phases of Iron Oxide Nanoparticles for Synthesis

Iron oxide contains sixteen refined phases Magnetite (Fe3O4), hematite, maghemite, goethite, akageneite, lepidocrocite, feroxyhyte, iron hydroxide, ferrihydrite, and wustite are a few of the various phases of metal oxide nanoparticles. The main iron oxide derivatives used to remove nitrate from water are magnetite and hematite, and small iron oxide nanoparticles with a large surface area, magnetic characteristics and more active sites are now a more promising method for treatment of nitrate removal from the water.[67] Particle surface area and the number of accessible active sites are crucial for the adsorption process.

Figure 5: Phases of iron

2.3 Methods of Preparation

Iron oxide nanoparticles have been produced using a variety of methods, and the final product has a mixture of divergent phases. In general, organic processes like co-precipitation and hydrothermal synthesis can be used to change the characteristics of iron oxide particles. However, it is not possible to make iron oxide nanoparticles on a large scale quickly without using intermittent and batch processes. There are many methods for the synthesis of iron oxide nano particles to execute proper shape, size and magnetize properties of particles and crystallinity.

2.3.1 Hydrothermal/Solvothermal Method

e phrase "hydrothermal/solvothermal process" refers to conducting chemical processes in solvents contained in vessels sealed shut where it is possible to raise the solvents' temperature to their respective critical points through heating while autogenous pressures are present. Employing water as the solvent makes a process "hydrothermal".[70] This phrase sometimes also refers to processes carried out in ambient circumstances. It is important to clarify that methods while hydrothermal

processes are ones in which water is used as the solvent, "solvothermal processes" involve using organics as the solvent.[71]

Following terminologies are use while explaining this method

- Precursor
- Mineralizer
- Additives

Precursors are reactants in the form of gels, solutions and/or suspensions. Mineralizers are inorganic or organic additions with large concentrations (e.g., 10 M) to adjust the pH of solutions.[72] Additives: organic or inorganic substances used in low amounts to regulate crystal shape or facilitate particle dispersion.

Most hydrothermal/solvothermal reactions take place in

- an autoclave,
- pressure vessel,
- or high-pressure bomb, which is a sealed reactor.

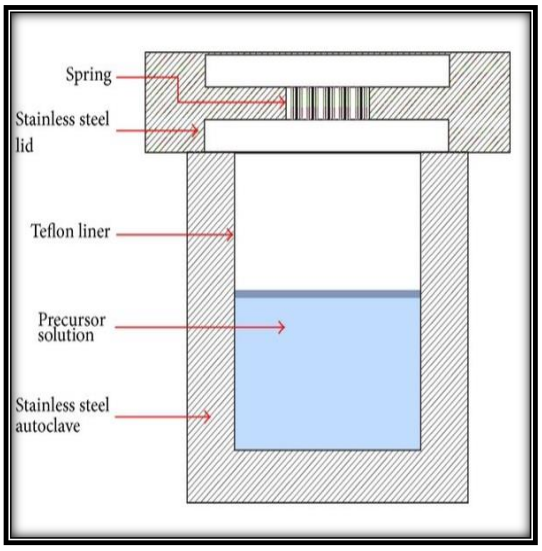

Figure 6: Schematic for hydrothermal/solvothermal model

Above is the Schematic for hydrothermal/solvothermal model [73]

Metal autoclaves are usually used for hydrothermal and/or solvothermal reactors with Teflon or alloy linings. They may also contain an additional beaker, tube or can made of gold, Teflon, silver or platinum to protect the body of the autoclave from the dangerously corrosive solvent which is kept at a high pressure and temperature. The

autoclaves occasionally have a Bourdon gauge affixed directly to them to monitor pressure and stirring accessories are included to reduce the concentration gradient inside of them.[72] An excellent hydrothermal/solvothermal autoclave should also be easy to assemble and disassemble, free of the possibility of leaks, and have sufficient operating life within the experimental pressure and temperature range.

Fundamental Processes of Hydrothermal and Solvothermal Crystal Growth Crystallization directly from solutions usually constitutes two steps:

- crystal nucleation and
- growth.

The final products might be manufactured with the necessary particle morphologies and sizes by adjusting the processing variables such as pH, temperature, additives, and concentrations of reactants. The growth and general nucleation rates are dependent on supersaturation and are the phenomena underlying the morphological and size control achieved through adjustment of the process variables.[70] The ratio of an organism's actual concentration to its saturation concentration in a solution is known as supersaturation. Although it is challenging to define the precise reaction equilibria due to the large number of species present in the hydrothermal/solvothermal solution, but there are many different models to determine this thing.[72]

As a result of their distinctive electronic, optical, mechanical, chemical and magnetic properties, which are mostly derived from the quantum confinement effect and large ratios of surface-to-volume, nanostructured materials with adjustable shape, size, tunable surface and crystallinity functionally have attracted significant research interest.[72] The most promising techniques for creating nanomaterials are thought to be the hydrothermal and solvothermal synthetic procedures. These techniques have several advantages, including the ability to produce vast quantities of nanomaterials at a low cost and the ability to produce highly crystalline nanocrystals with precise dimensions.[74] For the semicontinuous synthesis of materials with enhanced repeatability and excellent quality, microwaves and magnetic fields can be used in conjunction with hydrothermal and solvothermal processes.

2.3.2 Sol-gel Method

The sol-gel process is a technique used in materials science to create solid materials from tiny molecules. The technique is employed to create metal oxides, particularly

those of silicon (Si) and titanium (Ti). During the procedure, monomers are transformed into a colloidal solution (sol), which serves as the precursor for an integrated network (or gel) of discrete particles or network polymers.[75] Metal alkoxides are typical precursors. Ceramic nanoparticles are created via the sol-gel technique.

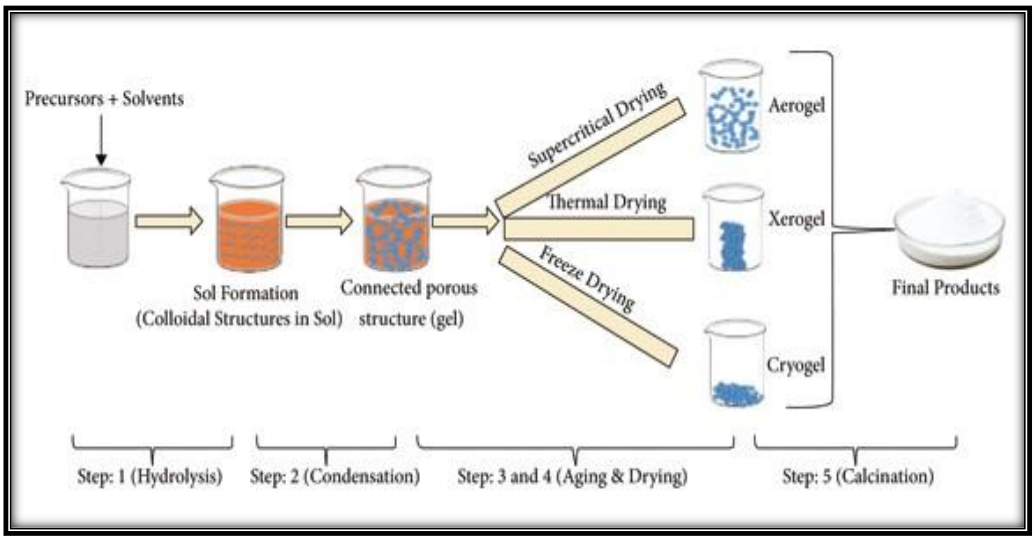

Figure 7: Steps of sol-gel method

Steps of sol-gel method [76] are given above.In this chemical process, a "sol" (colloidal solution) first develops before progressively evolving into the production of a gel-like diphasic system that has both a liquid phase and solid phase with morphologies ranging from discrete particles to continuous polymer networks. In the colloid's case, the volume fraction of particles (or particle density) may be so low that it may need a sizable amount of fluid to be initially removed to detect the gel-like qualities. There are numerous ways to achieve this.[77] The most straightforward approach is to wait for sedimentation to happen before pouring out the remaining liquid. Phase separation can also be hastened with the use of centrifugation.

Drying is necessary to remove the residual liquid (solvent) phase, and this process is sometimes accompanied by substantial shrinkage and densification. The distribution of porosity in the gel determines how quickly the solvent may be extracted.[78] During this stage of processing, modifications made to the structural template will undoubtedly have a significant impact on the final component's microstructure.

Then, to encourage additional polycondensation and improve mechanical characteristics and structural stability through final sintering, densification, and grain

growth, a heat treatment, or fire process, is frequently required. The fact that densification is frequently accomplished at a significantly lower temperature when using this technology as opposed to more conventional processing procedures is one of its key advantages.[79]

The precursor sol can be either cast into a suitable container with the necessary shape (e.g., to get monolithic ceramics, glasses, fibers, membranes, aerogels) or deposited on a substrate to form a film. It can also be used to create powders .

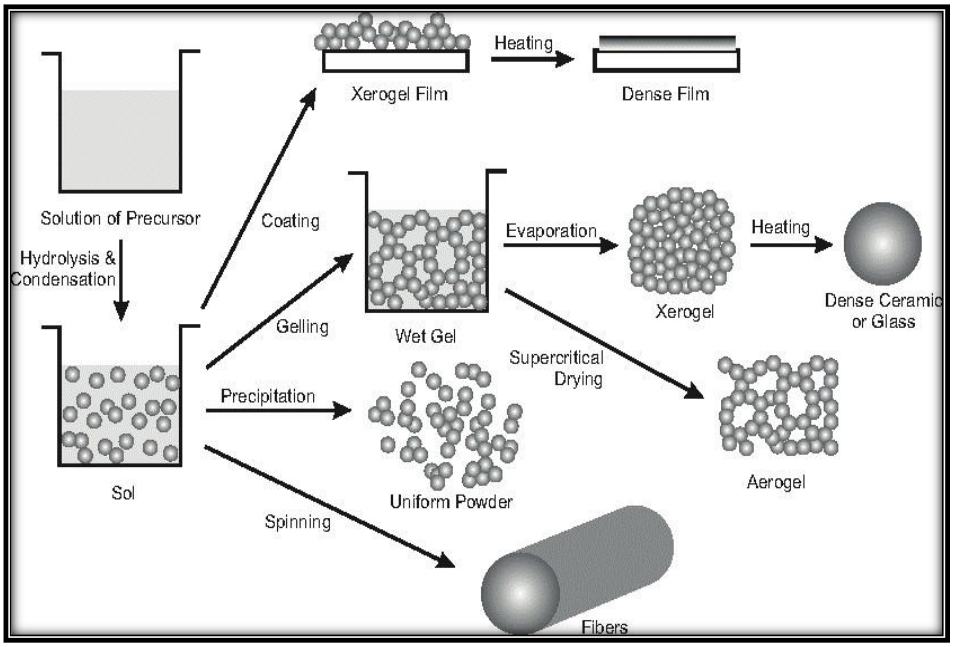

Figure 8: Schematic for sol-gel procedure

Organic dyes and rare earth elements, for example, can be added in very minute amounts to the sol and still end up evenly scattered in the result.[79] It can be used to make very thin films of metal oxides for a variety of uses or as an investment casting material in the processing and manufacture of ceramics. Materials made from sol-gel have a wide range of uses in technologies related to optics, electronics, energy, space, (bio)sensors, medicine (like controlled medication release), reactive materials, and separation.[76]

2.3.3 Co-precipitation Method

Coprecipitation is a frequent process used to create NPs, such as Fe3O4. This method can be used to create shells on prefabricated cores in addition to preparing NPs. The characteristic that various salts have varying degrees of solubility in water is exploited in the usual coprecipitation reaction. Two or more salts that are soluble in water are

utilized as reagents in reactions.[80] In the liquid phase, one or even more salts that are insoluble in water are created. Precipitation occurs when this product's concentration exceeds its solubility product value in the reaction medium. The freshly generated ions construct the shell by precipitating on the surfaces of the core instead of just dissolving in the solution.

Coprecipitation (CPT), also known as co-precipitation, occurs when chemicals that are typically soluble under the conditions used are carried down by a precipitate. Like this, coprecipitation in medicine refers to the selective precipitation of an unattached "antigen together with an antigen-antibody combination."[81]

Following are the three main mechanisms involved co-precipitation method

- Inclusion.
- Occlusion.
- Adsorption.

When an impurity occupies a lattice site in the crystal structure of the carrier, a crystallographic defect called an inclusion (incorporation in the crystal lattice) result. This can happen when the ionic radius and charge of the impurity are identical to those of the carrier.

An impurity that is either weakly or strongly bonded (adsorbed) to the surface of the precipitate is referred to as an adsorbate.

When an adsorbate impurity becomes physically stuck inside the crystal as it develops, it results in an occlusion.[82]

Different parameters like shape, size, morphology depends upon variable parameters like:

- Reaction temperature and other conditions
- pH value of the reactants
- Ionic strength of the reactants used
- Fe2+ /Fe3+ ratio
- Types of salts used like chlorides, sulphates, nitrates, carbonates etc.

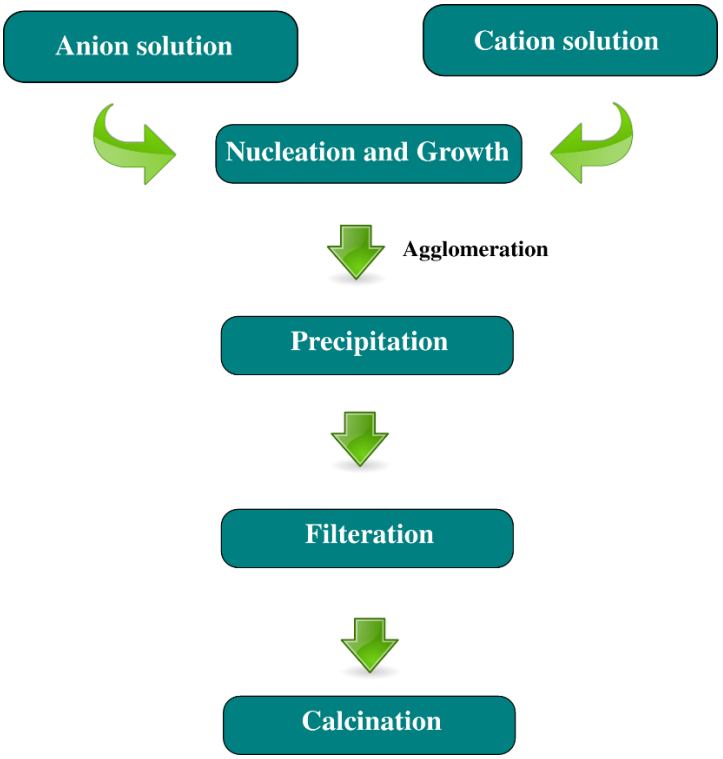

Figure 9: Stages of co-precipitation method

Iron oxide nanoparticles are typically created by adding base to aqueous iron salt solutions with an inert environment when they are elevated or at ambient temperature. Following is a description of the iron oxide precipitation reaction that results from this approach.

$$Fe^{2+} + 2O^{-} \rightarrow Fe(OH)_2$$

$$Fe^{3+} + 3O^{-} \rightarrow Fe(OH)_3$$

the overall reaction is

$$Fe(OH)_2 + Fe(OH)_3 \rightarrow Fe_3O_4 + 4H_2O$$

According to the reaction thermodynamics, an absolute precipitation of iron oxide NPs should be assumed to occur between pH values of 9 and 14, and the kind of salt is indicated by the letter "M," which might be either Fe2+, Co2+, Mn2+, Ni2+, Zn2+, Mg2+, or Cu2+. [80]

$$M^{2+} + 2Fe^{3+}\ 8(OH)^{-} \rightarrow MFe_2O_4 + 4H_2O$$

2.3.4 Thermal Decomposition Method

Thermolysis, commonly referred to as thermal decomposition, is a synthetic decay brought on by high temperatures. For this approach to work, heat is typically needed to break the compounds' electrovalent connections, which causes decay with an exothermic reaction.[83] It is particularly the most efficient method for creating due to the magnetic nanoparticles, which will allow us to finely modify the diameter of the particles. Usually, "heating up" and "hot injection" are the two methods that can be used to accomplish this. The heating-up process is represented by the steadily rising temperature of a pre-blended solution containing precursor chemicals, solvent, with surface agents at a specific temperature. Nanoparticles will start to expand and cluster at this temperature.[84] nonetheless, mixing analytes with a hot surfactant Hot-injection technique is a proven solution that allows for quick, homogenous nucleation and regulated development. Concisely, both procedures are founded on the same idea, namely heating.[85]

2.3.5 Micro-Emulsion Method

Surfactants, an amphiphilic molecule, are used in three phases of this approach, which is mostly employed to create uniform magnetic nanoparticles. This transparent procedure spreads a microdroplet of water into the monolayer molecules of the surfactant in a non-aqueous or continuous phase (oil). If a metal salt that is water soluble is added to the microemulsion's liquid phase, it will inhabit an oil-surrounded droplet in the liquid phase. The droplet is kept stable by the surfactant contained in it, which also helps to lower surface tension in the immiscible and continuous phase. They are also monitoring the micellization, which can disrupt the formation of magnetic iron oxide nanoparticles.[86]

When two similar micro emulsions are created with A solubilized in the aqueous phase of the first micro emulsion and B solubilized in the aqueous phase of the second micro emulsion, these droplets constantly collide, unite, and break apart to produce precipitate "AB," which will completely occupy the aqueous phase of the micro emulsions.

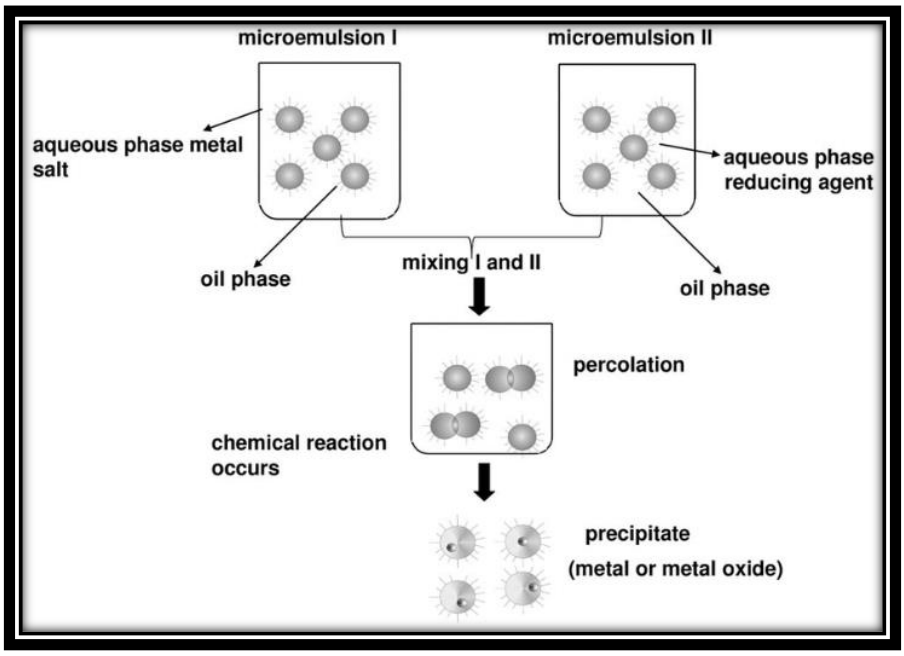

Figure 10: Micro-emulsion method

The size of droplets can be changed by surfactants with various concentrations and dispersed phases. Lamellar phase, continuous micro emulsions, cylindrical and spherical self-assembled structures are just a few examples. When compared to the magnetic nanoparticles made using Massmart's method, the micro emulsion method produces smaller particles.[86] Due to the lower reaction temperature, the main drawback of this method is the extremely poor crystallinity of nanoparticles on a wide scale.

2.3.6 Flow Injection Method

The flow injection method operates on the earlier tenet. It is a homemade system with Teflon lining, an injection valve, and multiple channel pumps. To give reproducible microinjections, a valve was employed.[87] Particles have been created using the zone of reaction restraint in different matrixes, such as emulsions, to vary their morphology and have a small dispersion. However, a specific reactor design can function as another matrix confinement. For the manufacture of magnetic iron oxide nanoparticles, a unique method is flow injection synthesis (FIS). Using a capillary reactor and laminar flow, the FIS approach involves intermittent or constant stirring of the reagents. The condition of laminar and plug flow, elevated stirring uniformity, and the potential for precise process control are some benefits of the FIS method.[88] The iron oxide magnetic nanoparticles display a narrow size distribution when the impact of environmental factors and chemical specifications were analyzed.

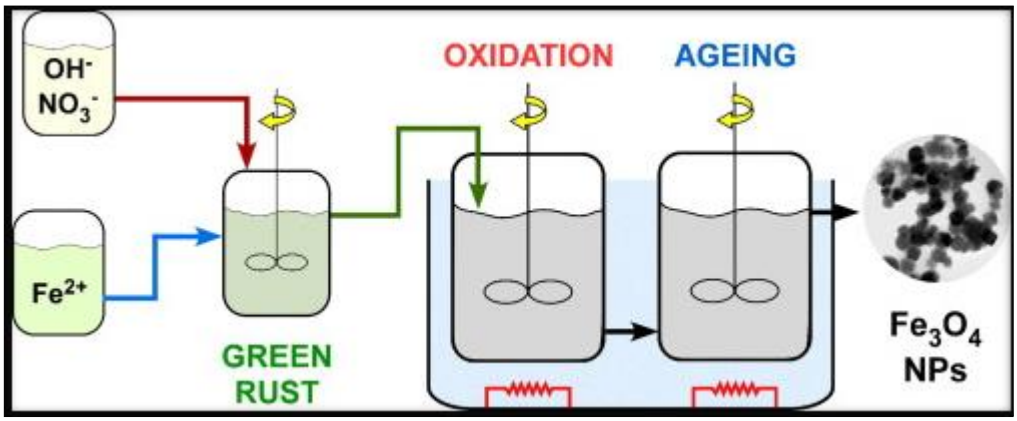

Figure 11: Procedure for flow injection method

2.3.7 Polyol Method

By employing this technique at a reasonable temperature, uniform magnetic nanoparticles can be easily manufactured.[89] Several precursor chemicals, including oxides, nitrates, and acetates, were used in this process, either in a dissolved condition or in a suspended state. It is a flexible synthesis technique that is best suited for producing massive clusters of iron oxide nanoparticles with a wide variety of potential sizes.[90] Based on the precursor used, the reaction temperature, the reaction duration, the type of solvent used, and the surfactant utilized, this sort of feature can be identified. Polyol is a particularly helpful way to create Nano crystalline substances or alloys.[89]

2.4 Iron Oxide Coated materials

The removal effectiveness was significantly increased by the large surface area and increased contamination activity of the small size particles. However, it is difficult to extract tiny particles. Since many metallic nanoparticles are tiny powders, they must be properly separated. Additionally, due to their poor hydraulic conductivity, these types of particulates cannot be used in column tests. Therefore, it is necessary for iron oxide nanoparticles to increase their surface area and conductivity coating. A hybrid sorbent that incorporates iron oxide scatter all over the polymeric porous bed has been employed in surface chemistry to increase the stability of the particles. The ability of NPs to disperse is improved by the coated iron oxide NPs moistened solution, but it is also severely inhibited the iron leaching into the solution.

While choosing a supporting surface following are some factors to consider

- Material availability

- Active sites present on the surface
- Nature
- Chemical stability
- Environmental hazards
- Cost

Rocks, sand, polymers, and ceramics are examples of porous, affordable, and readily accessible materials.

2.5 Application of Iron Oxide Nanoparticles

Fe oxide nanoparticles (NPs) have undoubtedly been widely used as very energetic catalysts in a variety of acid-base and oxidation/reduction processes. Compounds based on iron oxide have been regarded as the most effective and affordable materials for environmental catalysts.[91] Due to their high item collection ratio and high receptivity, iron oxide nanoparticles have been shown in recent studies to be more productive than conventional large-sized iron oxide.[84]

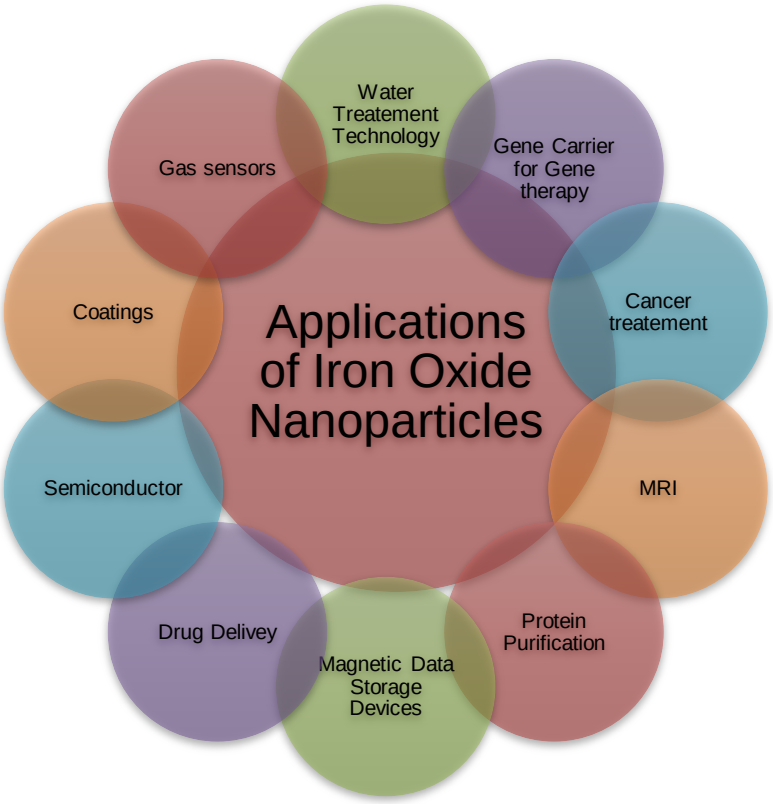

Figure 12: Applications of iron oxide nanoparticles

2.6 Hybrid Iron Oxide and Chitosan Beads

Chitosan (CS) is a new polymeric substance that has just come to be recognized for its extensive use in a variety of applications. It has a few distinguishing qualities, such as being biocompatible, nontoxic, and biodegradable, among others.[92]

Additionally, chitosan's unique and unexpected qualities, such as its low specific gravity, weak mechanical strength, poor solubility, agglomeration etc., made it more appropriate for adsorption. [93]As a result, it has been widely employed in applications based on the removal of environmental pollutants, such as the removal of heavy metals or dyes from contaminated water that may be used for drinking or industrial purposes.[92] In that case, chitosan might be employed in a mixed state with other materials to gradually improve these unexpected qualities.

Chitosan polymer matrix and dispersed phase of magnetic nanoparticles in iron oxide make up hybrid magnetic iron oxide impregnated with chitosan. Due to its exceptional mechanical strength, chemical, and biological qualities, chitosan has been a key component of magnetic particles. Due to its biodegradability, biocompatibility, low cost, and ease of availability, chitosan is the optimum material to produce magnetic polymeric material[94]. The repeating glycosidic residue contains two hydroxyl and one amino group, which aids in the creation of a suitable matrix to produce magnetic polymeric material.

The effectiveness of magnetic chitosan beads has stimulated scientific inquiry into a variety of potential applications. The use of magnetic iron oxide chitosan beads in a variety of industries, including wastewater treatment, biomedical (drug administration, bone regeneration, artificial muscles, anti-cancer emboli-therapy), environmental research (pollutant removal), and analytical (separation, biosensors, fluorescence probs) Chitosan is a cheap, environmentally benign, and reusable material that has a higher adsorption capacity and faster rate of adsorption than other adsorbent magnetic materials. Magnetic material typically clusters but does not because of the encircling polymeric substance

To improve their chemisorption capacity, iron oxide nanoparticles can be coated with biomaterials like chitosan. Chitosan is a widely accessible, non-toxic, and biocompatible polymer that can be easily produced from crabs, lobsters, shrimp, and other crustaceans[95]. Pure chitosan has, up until this point, been found to perform

more productively than chitin (precursor). Because chitosan has an NH group on it, chemisorption of harmful heavy metal ions will be promoted, and eventually these metal ions will be removed from wastewater.[96]

Iron oxide nanoparticles will also become less hazardous and environmentally friendly after being coated with chitosan, making it simple to utilize them to remove heavy metal ions from drinking water[97]. By combining hybrid iron oxide nanoparticles and chitosan composites in this way, we can create a solution that is both efficient and affordable. This technology can be utilized on a broad scale to remove water pollutants.[98]

Chapter: 3

Materials and Methods

3.1 Chemicals Required

Following are the chemicals required for the synthesis of magnetic nanoparticles, beads, and Synthetic Model water

- Sodium hydroxide (NaOH)
- Iron (III) Chloride Hexahydrate ($FeCl_3.6H_2O$, Duskan reagents)
- Iron (II) Chloride Tetrahydrate ($FeCl_2.4H_2O$, Duskan reagents)
- Sodium Nitrate ($NaNo_3^{2-}$)
- Chitosan ($(C_6H_{11}NO4)_{n,}$ sigma Aldrich.)
- Polyvinylpyrrolidone (PVP)
- Sodium Chloride (NaCl)
- Magnesium Chloride ($MgCl_2$)
- Sodium Sulphate ($NaSO_4^{2-}$)
- Ethylene glycol (MW 62.07, sigma Aldrich.)
- Hydrochloric Acid (HCl)
- Ammonia (NH_4OH-32%, Merk)
- Acetic Acid (CH_3COOH) (glacial 99-100%)

3.2 Synthesis of Magnetic Nanoparticles

The co-precipitation process was used to create the nanoparticles. 100 ml of deionized water were mixed with 8mmol $FeCl_3.6H_2O$ and 4mmol $FeCl_2.4H_2O$ to dissolve them at 20°C. Then, 5 ml of aqueous ammonia hydro oxide solution (NH_4OH-32%) was promptly added while stirring. The precipitates were allowed to settle in the bottom of the beaker after the system reached the precipitation state. The liquid supernatant was decanted after precipitation. The precipitation was removed until the pH was neutral.[74] The cleaned precipitates were then separated, dried for an overnight period at 60°C, and crushed into a fine powder. To create a steady dispersion of nanoparticles in water, the particles were subjected to an acid treatment. After precipitation, the particles were dried and crushed to create water-dispersible magnetic nanoparticles. [66]

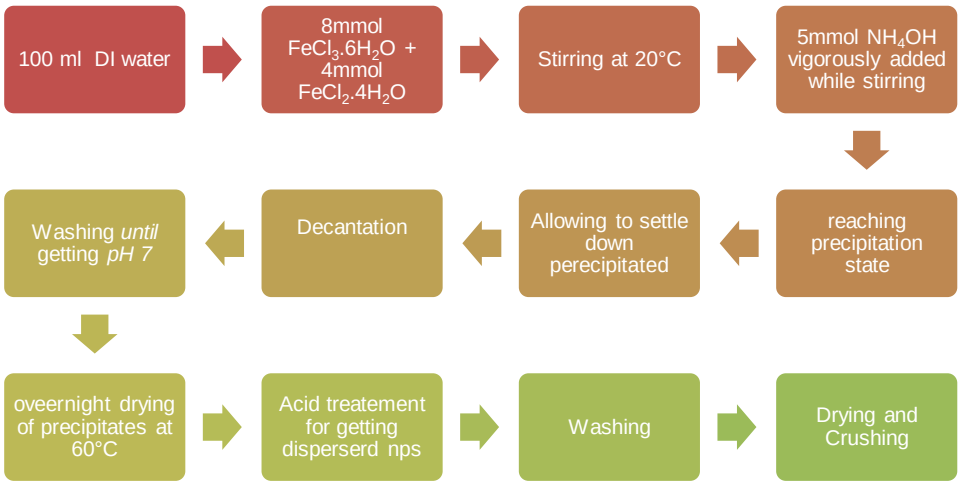

Figure 13: Block diagram for synthesis of iron oxide nanoparticles

3.3 Synthesis of Iron Oxide Impregnated Chitosan Beads

Iron oxide embedded chitosan beads (IECB) were synthesized by using embedding method. Whereas iron oxide NPs were prepared by using method of Co-precipitation prior to this. To create hybrid beads, combine 2.6% v/v acetic acid in a 50ml solution with 3.5grammes of chitosan while stirring continuously for 4 hours at 450 rpm. Add 1g of Fe_3O_4 nanoparticles to the viscous clear solution once it has become viscous and agitate it once more to create a viscous homogeneous solution. This solution should be sonicated for five minutes at room temperature to remove air. Now, a syringe was used to add the resultant slurry of chitosan-iron oxide solution drop by drop into a solution of 1 mol/L NaOH while stirring continuously. Then, hybrid chitosan-iron oxide beads were removed from the NaOH solution and repeatedly submerged in water until the filtrate's pH was neutral. In the end, beads will be dried in an oven set to 65°C for four hours.[98, 99]

Figure 14: Block diagram for synthesis of iron oxide embedded chitosan beads

3.4 Characterization Techniques

The following approaches were used to characterize iron oxide nanoparticles and iron oxide nanoparticle-impregnated chitosan beads.

- X-ray Diffraction (XRD)
- Ultraviolet- Visible (UV-Vis) Spectroscopy
- Fourier Transform Infrared (FTIR) Spectrometry
- Scanning Electron Microscopy (SEM)
- Brunauer-Emitter-Teller (BET)
- Contact Angle

3.4.1 X-ray Diffraction (XRD)

The experimental science known as X-ray crystallography employs incident X-ray beams to diffract into numerous distinct directions to identify the molecular and atomic structure of crystals. An image of the density of electron within the crystal can be created in three dimensions by determining the angles and intensity of these diffraction patterns. [100]The average locations of the atoms within the crystal, along with their chemical bonds, degree of crystallographic disorder, and other details, may all be calculated from this electron density.

X-Ray Diffraction is used to study the crystalline structure of materials, essential information can be decoded by the XRD such as:[101]

- composition of solid material.
- Crystallinity.
- grain size.
- lattice parameter
- Atomic arrangement
- Preferred orientation
- Phase composition
- Epitaxy

The wavelength of XRD is approximately (1Å), larger than gamma rays (γ-rays) although shorter as compared to the ultra-violet (UV).
X-ray diffraction is based on two elements:

- constructive interference of monochromatic X-rays

- a crystalline sample.

These X-rays are generated by:

- cathode ray tube
- filter to produce monochromatic radiation
- collimated to concentrate and directed toward the sample.

W.L. Bragg thought that the X-ray diffraction from a crystal was a problem of X-ray reflection from the atomic planes of the crystal in line with the laws of reflection to explain the diffraction of X-rays.

Mathematically Bragg's Law Equation can be written as,

$n\,\lambda = 2dsin\Theta$

- n is order of reflection
- ƛ is wavelength of X-rays
- d is characteristic spacing of crystal plane
- θ is the angle formed between normal plane and incident beam

Braggs law is used to understand the process of diffraction. For measuring the crystallite size Debye-Scherer equation was used, Mathematically it can be written as,

- D=Kλ/ (β cos θ)
- D is average cryatalline size
- β is fullwidth at half maxima
- λ is wavelength of X-rays
- θ is Braggs angle
- K is Debye-Scherrer constant

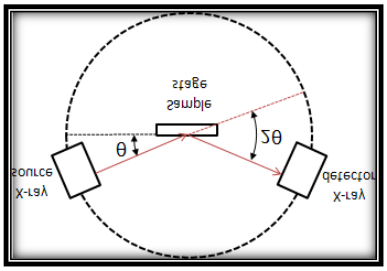

Figure 15: Bragg's law

X-ray diffraction (XRD) is one of the maximums drastically used strategies for the characterization of NPs. Typically, XRD affords statistics concerning the crystalline structure, nature of the phase, lattice parameters and crystalline grain length. The latter parameter is anticipated via way of means of the usage of the Scherrer equation the usage of the broadening of the maximum severe top of an XRD dimension for a particular sample. A gain of the XRD strategies, typically achieved in samples of powder form, commonly after drying their corresponding colloidal solutions, is that its outcomes in statistically representative, volume-averaged values. database. However, it is not always appropriate for amorphous substances and the XRD peaks are too large for debris with a length beneath three nm. Upadhyay et al. decided the common crystallite length of magnetite NPs the usage of X-ray line broadening, and it turned into determined to be withinside the variety of 9–fifty-three nm. The broadening of XRD peaks turned into especially because of particle/crystallite length and lattice traces apart from instrumental broadening [78]The XRD-derived length is commonly larger than the so-referred to as magnetic length, because of the truth that smaller domain names are found in a particle wherein all moments are aligned withinside the identical direction, with the particle is single domain

3.4.2 Ultraviolet- Visible (UV-Vis) Spectroscopy

UV spectroscopy or UV-visible spectroscopy (UV-Vis or UV/Vis) refers to the reflectance spectroscopy or adsorption spectroscopy of the ultraviolet and entire near-visible parts of the electromagnetic spectrum. As an affordable and easy to perform methodology, it is often employed in various theoretical and practical applications. It is important for the sample to be a chromophore and be able to absorb in the UV-Visible range. Absorption spectroscopy can be used to enhance fluorescence spectroscopy. In addition to the measurement wavelength, variables of interest include absorbance (A), transmittance (%T), and reflectance (%R), as well as how they change over time.

The UV-Visible Principle: The foundation of spectroscopy is the absorption of visible or ultraviolet light by chemical substances, resulting in distinguishing spectra. The interaction of light and matter form the basis of spectroscopy with a spectrum being created once a substance absorbs light via excitation and de-excitation processes.

For the quantitative determination of a variety of analytes or samples, including transition metal ions, highly conjugated organic compounds, and biological macromolecules, UV/Vis's spectroscopy is frequently utilized in analytical chemistry. Although solids and gases as well as liquids can be examined by spectroscopy.

According to the Beer-Lambert equation, the concentrations of the absorbance values in the solution and the route length are exactly proportional to the absorption of a solution. Thus, the concentrations of the absorbance in a solution can be determined using UV/Vis's spectroscopy for a constant route length.

The Beer-Lambert law is most frequently applied to the method to quantitatively quantify the concentration of an absorption in the solution.

Mathematical equation for this can be written as

$$A=\text{Ɛ}cL$$

- A is absorbance
- Ɛ is Beer Lambert constant which represent molar absorptivity
- c is concentration of absorbing specie
- l is path length through the sample

The main drawback of using a UV-Vis spectrometer is the time required for setting it up. Setup cannot be overlooked, and the area of choice needs to be cleared of outside light, electrical noise or any impurities that could possibly impact the spectrometer's accuracy of measurement. Solid particles suspended in liquid as a sample would be tricky to work with as UV-vis spectroscopy performs well with solutions and liquids, but the data will be significantly skewed since the sample scatters light more than it absorbs.[92, 101] Although it is uncommon, most UV-vis devices can evaluate solid samples or solutions using a diffraction apparatus. The most effective equipment for liquid and solution analysis are UV-vis ones.

3.4.3 Fourier Transform Infrared (FTIR) Spectrometry

An infrared spectrum of an object's absorption or emission can be obtained using the Fourier-transform infrared spectroscopy (FTIR) method. High-resolution spectral data are concurrently collected over a broad spectral range by an FTIR spectrometer. In comparison to a diffraction spectrometer, [39]which measures intensities over a limited range of wavelengths at a time, this offers a substantial advantage.

With a wavelength range of 400 cm to 4000 cm, the Perkin Elmer Spectrum 100 Spectrometer was used to perform the Fourier transform infrared. The raw data of infrared radiations can be transformed into the actual spectrum using the Fourier transform method. [98]FTIR can be used to analyze samples in both qualitative and quantitative ways, regardless of whether they are organic or inorganic. The use of IR to distinguish between various functional groups and identify bonds is incredibly beneficial.[102]

This approach uses a light of multiple frequencies at once instead of monochromatic illumination at the sample, and the absorption of light by the sample is computed. [92]Additionally, alternative frequency combination can be used in this technique to obtain a second data point. This process will also repeatedly occur during the same period. All this data will be promptly analyzed at the computer's back end, and the absorption of the spectrum will be measured for each wavelength.[103]

Most materials' ability to perform the needed function is controlled by subtle differences in their physical and chemical make-up.[100] Additionally, studying the chemical composition at the microscopic scale and how it relates to the material's microscopic qualities is useful for improving the material's performance.

In the FTIR technique, a sample is placed in an IR beam, which absorbs some radiations that correspond to molecular vibrational frequencies whereas the specimen itself transmits all other radiations. The frequency of radiant energy that were both absorbed and transmitted, displayed as a spectrum. It is possible to identify a [104]substance because distinct vibrational frequencies of various materials each have their own spectrum. [55]

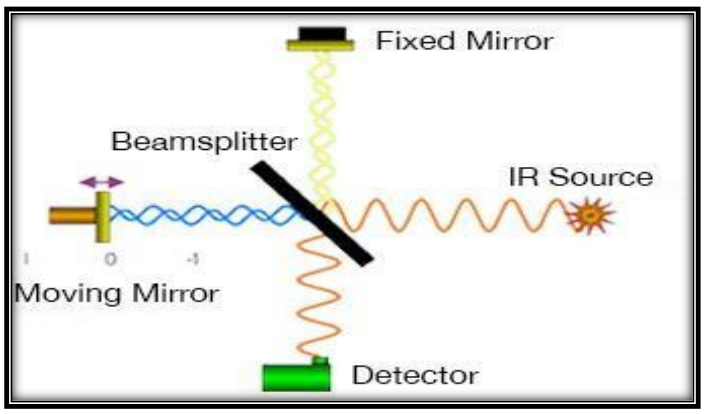

Figure 16: FTIR Schematic

3.4.4 Scanning Electron Microscopy (SEM)

Scanning electron microscopy is known as SEM. It is a microscope that creates a more precise image by interacting with the surfaces of the subject being studied with a beam of highly concentrated electrons. When these electron beams come back, they transmit information regarding the precise structure of the materials. They make known the outward structure, chemical makeup, and orientation of the constituent materials that make up the material.[105]

In a SEM, accelerated electrons with high levels of kinetic energy interact with the sample. When the incident electrons are decelerated in the solid sample, energy is lost as a variety of signals created by electron-sample interactions. These signals are made up of secondary electrons (which create SEM images), backscattered electrons (BSE), diffracted backscattered electrons (EBSD), photons (which include continuum X-rays and characteristic X-rays used for elemental analysis), visible light, and heat. Backscattered electrons are utilized to reveal disparities in composition in multiphase materials, while secondary electrons are frequently employed to display morphological and topography on samples. As the high energy electrons revert to lower energy states and produce X-rays with a set wavelength (determined by the difference of energy state of electrons in various shell for a given element), [69]X-ray production is also observed. As a result, each component in a material that the electron beam "excites" emits distinctive X-rays.[78]

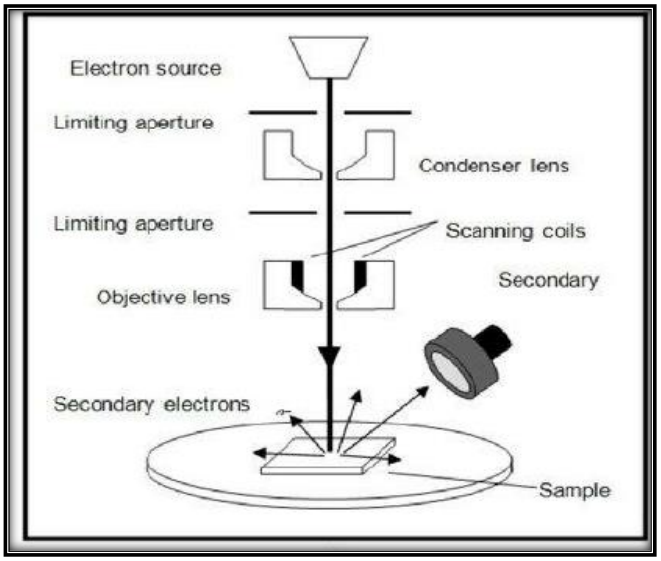

Figure 17: Components of SEM

SEM includes following components.

- Electron Source ("Gun")
- Electron/ Magnetic Lenses
- Sample Stage
- Detectors for all signals of interest Display / Data output devices
- Infrastructure Requirements
- Power Supply
- Vacuum System
- Cooling system
- Vibration-free floor
- Room free of ambient magnetic and electric fields Applications

SEM also provides knowledge about following things along with the surface and internal morphology of the materials.

For on-the-spot chemical analysis, elemental maps

- Identification of phases based on qualitative chemical analysis and/or crystalline structure. Discrimination between phases.
- Compositional maps.
- Also used to measure size precisely to 50 nm.

There is no comparison for this instrument given the variety of applications it has in the research of domains requiring the characterization of substances are dependent on the SEM. Substances depend on the SEM. Most SEMs have user-friendly, "intuitive" interfaces allow them to be easy to use. There is little preparation required for the sample for many applications. Capturing data is also quick for many applications and is usually below 5 minutes per picture for BSE, spot EDS and SEI studies. Modern SEMs have the added advantage of producing data in portable digital formats.[53]

Even with all the benefits, there are a few slight drawbacks to employing SEM. Examples include the requirement that samples should be solid and fit inside of the microscope chamber. Roughly 10 cm is the maximum horizontal dimension size and the vertical dimension size is rarely above 40 mm. SEM EDS detectors cannot detect light elements such as H, Li and He and there are devices that cannot detect elements of atomic numbers less than 11 (Na). Noticeably light elements (H, He, and Li) cannot

be detected by SEM EDS detectors, and many devices cannot detect elements with atomic numbers below 11. (Na).[52] Most SEMs use solid state x-ray detectors (EDS), which are quick and simple to operate but have subpar energy resolution and element sensitivity. Electrically insulating samples require the application of an electrically conductive coating.[101]

3.4.5 Brunauer-Emitter-Teller (BET)

The Brunauer-Emmett-Teller (BET) theory is a key analytical tool for the measurement of the specific surface area of materials. It seeks to explain the physical adsorption of gas molecules on a solid surface. Physical adsorption or physisorption is a term that is frequently used to describe the observations. In the Journal of the American Chemical Society, Stephen Brunauer, Paul Hugh Emmett, and Edward Teller published their idea in 1938. The BET theory is applicable to multilayer adsorption systems that typically employ a probing gas (referred to as the adsorbate) that does not chemically react with the adsorptive (the substance that the gas adheres to; the gas phase is referred to as the adsorptive).

The most popular gaseous adsorbate for exploring surfaces is nitrogen (s). Due to this, routine BET analysis is often carried out at N2's boiling point (77 K). To quantify surface area at various temperatures and measurement scales, other probing adsorbates are also used, albeit less frequently. These consist of water, carbon dioxide, and argon. Quantities of specific surface area obtained by BET theory may be affected by the adsorbate molecule used and its adsorption cross section because specific surface area is a scale-dependent feature with no one true value specified.

The specific surface area is calculated using the theory of gas molecule monolayer synthesis on a solid surface. The experimental adsorption isotherm is then converted into a BET plot using the BET model, which employs a linearized version of the BET equation, allowing the monolayer volume to be calculated. The total specific surface area expressed in m2/g is then calculated in this BET analysis using the gas molecule's cross section area and the monolayer volume. In addition to BET analysis, gas adsorption can be used to determine the presence of pores in terms of both pore volume and pore size distribution. Since capillary condensation in pores is pore size dependent, the pore size distribution can be calculated using the capillary condensation in pores principle. To cause condensation in bigger holes, a higher pressure is required. Like this, smaller holes are filled at lower adsorbing gas partial pressures.

The sample is pre-treated at a high temperature in a vacuum or a flowing gas before the measurement to remove any impurities. Pre-treatment settings must be adjusted to the qualities of the materials since too low or too high a temperature can negatively impact the BET surface area obtained from the subsequent BET analysis.

3.4.6 Contact Angle

The contact angle is the angle at which a liquid-vapor interface encounters a solid surface. It is typically measured through the liquid. Contact Angle measurements is a method to observe the properties of solid-liquid interface. It is the vital parameter to examine the wettability of surface. Wettability is control by two parameters.

- Percentage contact
- Surface energy

The Young equation is used to determine the moisture to liquid ratio of a solid surface. Every system has a different equilibrium contact angle with a particular solid, liquid, and vapor at a given temperature and pressure. However, it is frequently noticed in actual use of the dynamic phenomena known as contact angle hysteresis, which can range from the advancing (maximal) contact angle to the receding (minimum) contact angle.

These values allow one to compute the equilibrium contact which lies within them. The equilibrium contact angle displays the relative strength of the molecular interactions between liquid, solid, and vapor. The composition of the liquid and solid in interaction and the medium above liquid's free surface affects the contact angle. The solid surface is unaffected no matter how steeply it slopes in the direction of the liquid surface. Surface tension, which also affects temperature and liquid purity, has an impact upon this.

A contact angle of 0° indicates complete wetting if the liquid spreads equally across the solid surface. The surface is wettable when the angle is between 0 ° and 90 °. It is known as a hydrophilic surface. The surface cannot be wettable if the angle is between 90 and 180 degrees. It is water-repellent. It is an ultra-hydrophobic surface that is entirely liquid repellent if the angle clearly approaches the value of 180 °. The lotus effect is used to characterize this phenomenon.

The equipment for determining contact angle includes

- A light source with variable brightness
- A droplet syringe unit, an adjustable measuring stage
- A very quick video system with a camera and
- Adaptor.

Droplet from the syringe's stainless-steel needle fell and hit a solid surface. The droplet image was captured, and the drop's contact angle with the sample's surface was then measure

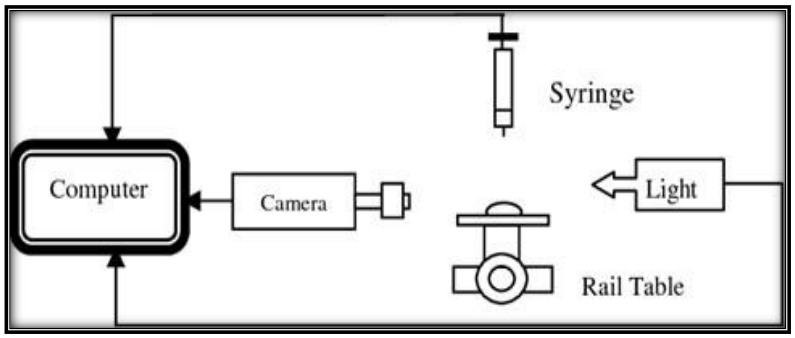

Figure 18: Schematic for contact angle measurement

Chapter: 4

Results and Discussion

4.1 X-ray Diffraction Spectroscopy

4.1.1 XRD Pattern of Iron Oxide Nanoparticles

XRD was done of the prepared iron oxide nanoparticle for the analysis of crystalline nature and structure of these particles. The XRD pattern of prepared nanoparticles is shown in Figure 19. The amorphous and crystalline nature was observed. The crystalline peaks of Fe_3O_4 were noticed at 2θ = 30.15°, 35.55°, 43.1°, 56.97°, and 62.55°, indexed to the characteristic plane (220), (311), (400), (422), (511), and (440) of Fe_3O_4 without impurities present in them as per reported in the previous literature. The peaks observed in the present analysis were at 2θ= 18.9° , 35.8° ,43.2°,56.9° and 62.72° indexed to the characteristic planes (311), (400), (422), (511), and (440), which confirms the presence of Fe_3O_4.

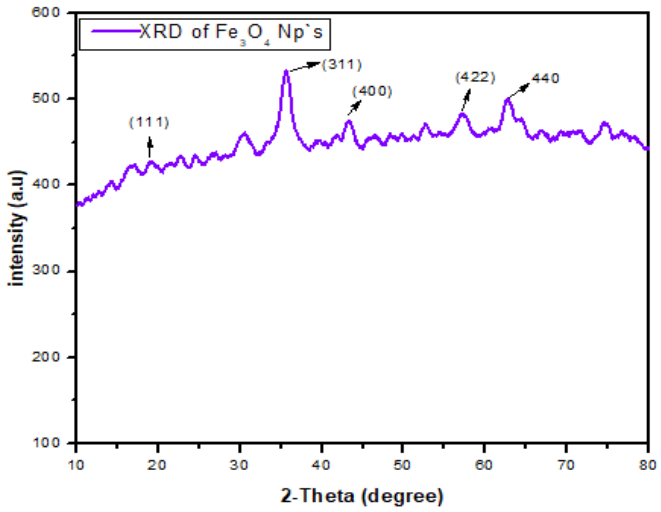

Figure 19: Graphical representation of XRD for Fe_3O_4Np's

4.1.2 XRD Pattern of Impregnated Chitosan Bead

XRD of the prepared chitosan beads was done for the analysis of crystalline nature and structural properties. The beads were prepared using the nanoparticles as shown in Figure 19 and 21. The pattern of these beads is shown in the graph below Figure 20. The characteristic peaks were noticed at 2θ= 35.2°, and 63.82° indexed with (111), (311) and (440) which shows the of the presence Fe_3O_4 and confirms the crystalline

nature of Fe_3O_4. The angle at 2θ= 18.9° with the index (111) confirms the presence of Chitosan in beads and confirms its semi crystalline nature. The results proved that the Magnetic Chitosan beads were synthesized properly without any damage to the structure of Fe_3O_4 nanoparticles.

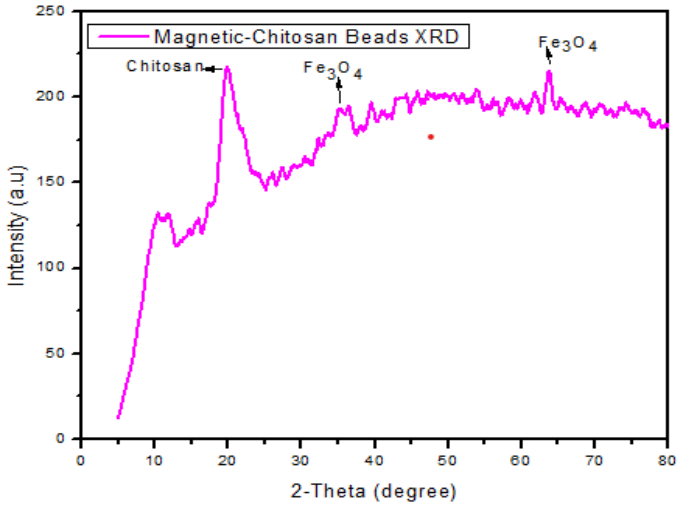

Figure 20: Graphical representation of XRD for Magnetic-Chitosan Beads

4.2 Scanning Electron Microscopy (SEM)

4.2.1 SEM of Iron Oxide Nanoparticles

The morphology of these iron oxide nanoparticles synthesized by the co-precipitation method was analyzed the scanning electron microscopy (SEM) shown in Figure 21. The images show that the surface of the nanoparticle is porous and rough which means each iron oxide nanoparticle is composed of numerous tiny particles. The spherical shape agglomeration was seen in these images. The steric action connected to the active sites on the surface of the nanoparticles is what causes this agglomeration. The agglomeration observed via SEM image is considered due to the magnetic interaction created by single iron oxide nanoparticle.

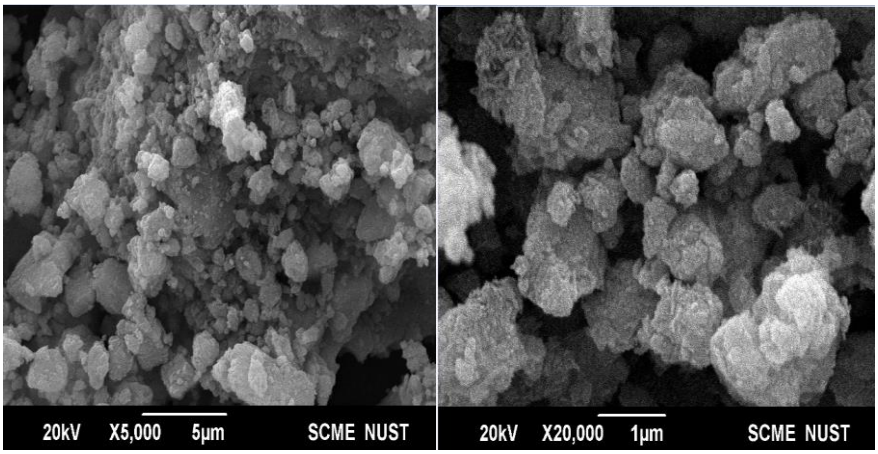

Figure 21: SEM images of iron oxide nanoparticles

4.2.2 SEM of Impregnated Chitosan Bead

The surface morphology analysis of iron oxide embedded chitosan beads was done by using scanning electron microscopy (SEM), Shown in Figure 22, by which it was determined that the shape of these beads is irregularly spherical with slightly porous and rough surface. The thickness of these magnetic chitosan beads varies from 1.09mm to 1.30mm. These results showed that these were the iron oxide coated chitosan beads. Iron Oxide NPs in chitosan have been observed in various folds on the surface of the bead; as a result, a sizable portion of the surface and several mobile sites have manifested on the outer surface. This sort of bead's morphology was most likely caused by the bonding of iron oxide NPs and pure chitosan chain groups (-NH2 and -OH).

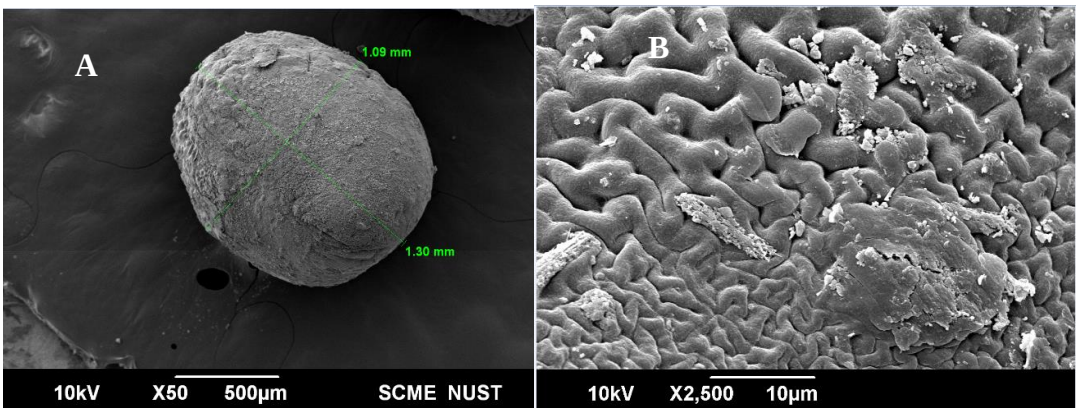

Figure 22: SEM images of impregnated chitosan beads

4.3 Fourier Transform Infrared (FTIR) Spectroscopy

4.3.1 FTIR of Iron Oxide Nanoparticles

The functional group analysis of the prepared nanoparticles was done by Fourier transform infrared (FTIR) spectroscopy shown in Figure 23. This FTIR analysis was performed from the wide range of intervals of wavelength (4000-400) cm^{1}. The broad band observed at 580 cm^{-1} and 630 cm^{-1} in the present analysis shows that it is due to pure metallic oxygen (Fe-O) functional group coordination bond and the peak produced at this point is due to the vibrational stretching of Fe-O bond. The peak shown at 1114 cm^{-1} is due to the presence of the ammine functional group and the stretching here is C-N for ammine. The Fe atoms were coordinated with the O atom from O-H group resulting in Fe-O The peaks observed at 2411 cm^{1},2652 cm^{1},2921 cm^{1} are due to the presence of alkyl and amide functional groups. The peaks observed at 3424 cm^{1} are due to the presence of secondary ammine functional group and give N-H and O-H

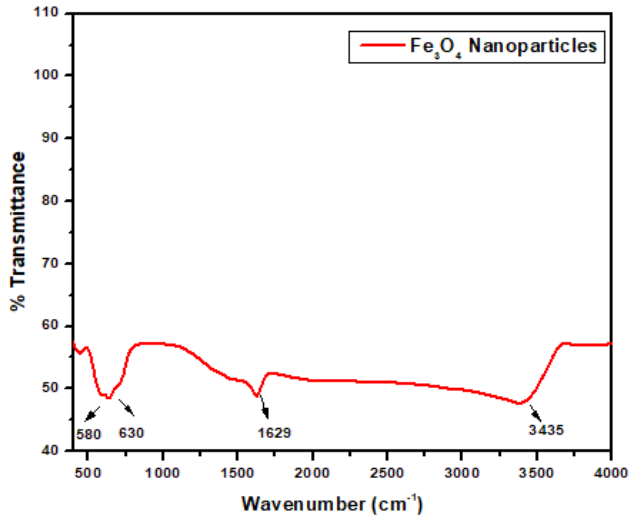

Figure 23: Graphical representation of iron oxide nanoparticles

4.3.2 FTIR of Impregnated Chitosan Bead

Functional group analysis of the prepared beads was done using FTIR as shown below in Figure 24. The spectrum range studies was from 4000 cm^{1} to 400 cm^{1}. The broad band observed at 616 cm^{-1} in the present analysis shows that it is due to pure metallic oxygen (Fe-O) functional group coordination bond and the peak produced at this point is due to the vibrational stretching of Fe-O bond. The peak shown at 1626 cm^{-1} is due to the presence of the ammine functional group and the stretching here is C-N and

includes N-H vibrations. The peaks observed at 3435 cm^{1} are due to the presence of secondary amine functional group and give N-H and O-H.

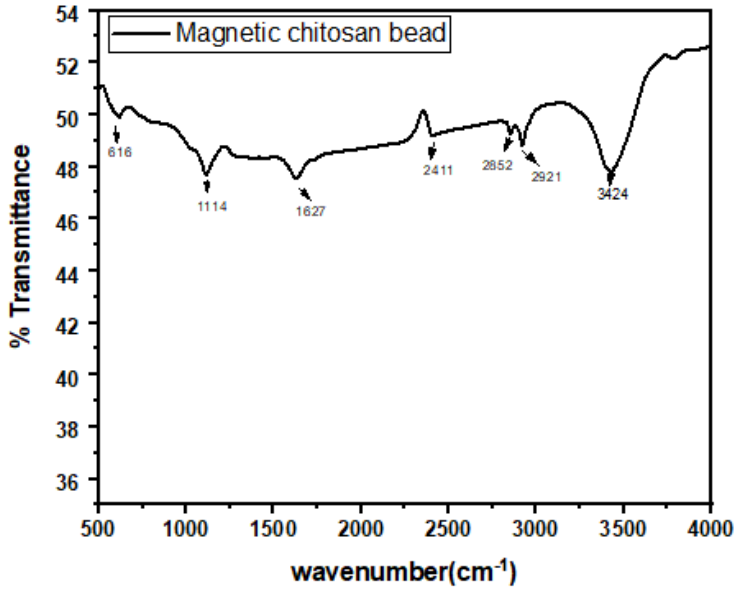

Figure 24: Graphical representation of FTIR for Magnetic Chitosan Beads

4.4 Adsorption Study

180 mg Beads were put into 1L solution of nitrate water for an adsorption experiment. For two hours, a mechanical shaker was used to stir continuously to extract the nitrate and absorb it onto the chitosan beads with iron oxide embedded in them. At a predetermined time, interval, samples were removed from the flask, and the concentration of nitrate was measured using UV-visible spectroscopy. Finally, a formula was used to determine the capacity of the adsorbent to bind nitrate.

Qe = (Co-Ce) *V/m

Here in this equation,

- Qe is adsorption capacity (mg/g)
- Co and Ce are initial and final concentrations (mg/l)
- V is volume of the mixture in liters (L)
- m is the weight of beads

Using UV-Vis's spectroscopy, we can determine that there is still 0.414 mg/l of nitrate in the water, which indicates that 93% of the nitrate has been removed in two hours. The following formula can be used to determine removal efficiency.

Removal efficiency (%) = ((Co-Ce)/Co) * 100

Here Co and Ce are the initial and final concentrations.

4.4.1 Adsorption Isotherm

Adsorption isotherm models, such as the Langmuir and Freundlich isotherm models, can be used to calculate the amount of the nitrate compounds on the beads from the solution at constant temperature.

4.4.1.1 Langmuir Isotherm Model

Table 3: Regression value of Langmuir isotherm model

Langmuir Model		
Q_{max} (mg/g)	K_L (L/mg)	R^2
5.291005	3.268837	0.99093

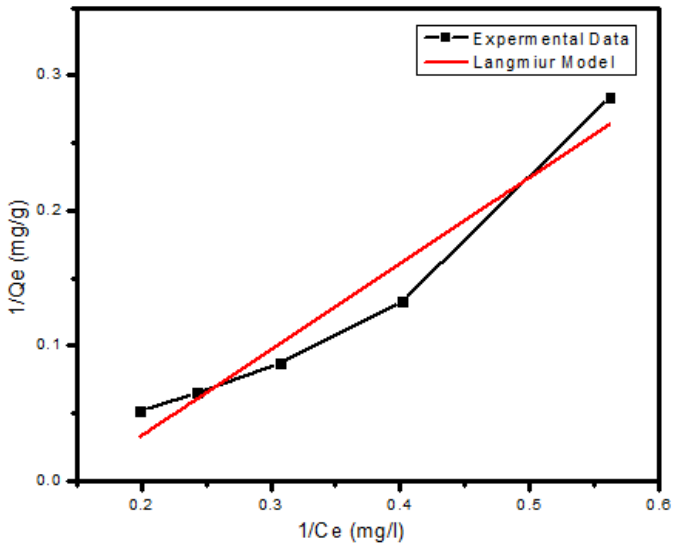

Figure 25: Graphical representation of Langmuir isotherm model

4.4.1.2 Freundlich Isotherm Model

Table 4: Regression value of Freundlich isotherm model

Freundlich Model		
K_f	N	R^2
0.91047	1.5699	0.98251

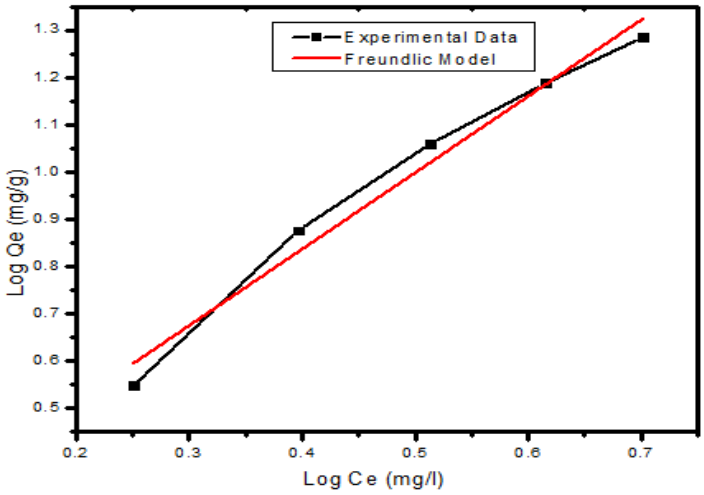

Figure 26: Graphical representation of Freundlich isotherm model

4.4.2 Adsorption Kinetics

With the help of the adsorption knight, i.e., pseudo-first order and pseudo-second order processes, the overall evaluation of the adsorption method is established.

4.4.2.1 Pseudo First Order Kinetic Model

Pseudo First Order		
Qe (mg/g)	K_1	R^2
3.211185	-2.4×10^{-4}	0.89485

Table 5: Regression value of Pseudo First Order Kinetic Model

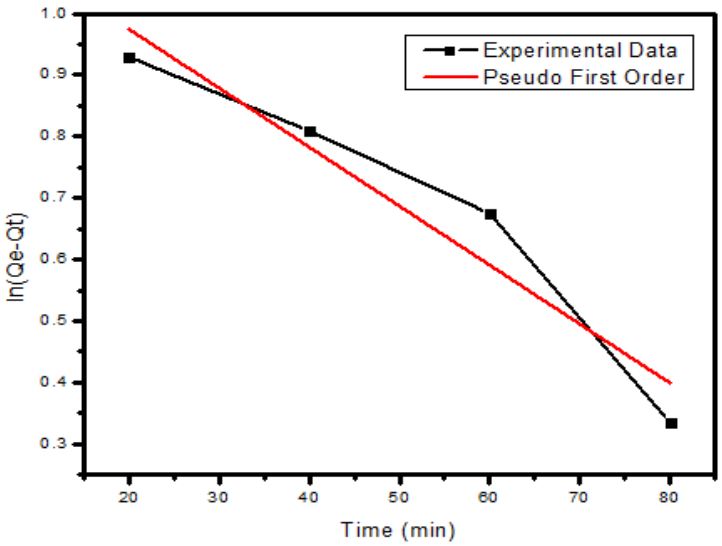

Figure 27: Graphical representation of First Order Kinetic Model

4.4.2.2 Pseudo Second Order Kinetic Model

Table 6: Regression value of Pseudo Second Order Kinetic Model

Pseudo Second Order Kinetic Model		
Qe (mg/g)	**K2 (h. g/mg)**	**R^2**
20.84636	15.852 x 10^{-4}	0.9955

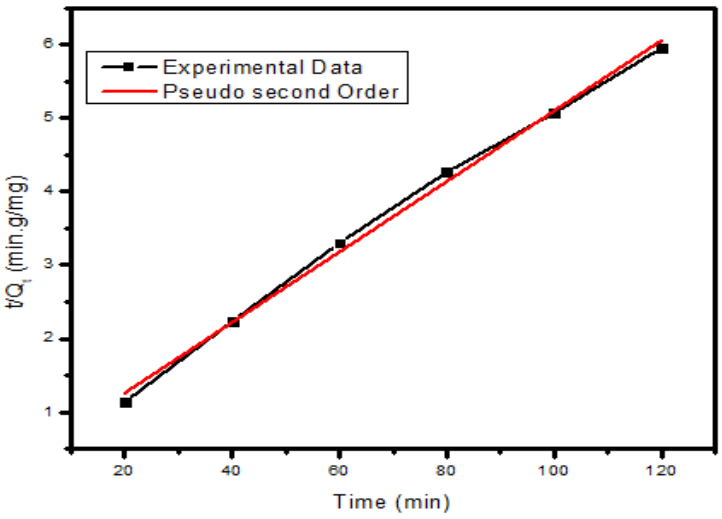

Figure 28: Graphical representation of Pseudo Second Order Kinetic Model

The graphs shows that the initial rate of bead adsorption was quite high due to the surface's high number of active sites and low resistance to mass transfer in the absence of adsorption. The value of R^2 demonstrates that this adsorption process complies with pseudo-second order kinetics, and it supports the model's assumptions that the adsorption process results from chemisorption by predicting performance across the entire range of studies. Pseudo-Firsts order cannot provide the perfection for the currently available preliminary data, as demonstrated by the value of R^2. Furthermore, less Nitrate-sorbent interaction, or physisorption, seems to be related to improved relevance of the pseudo first order.

4.5 Impact of Different Parameters

Impact of following parameters was studied for adsorption study:

1) Time 2) pH 3) Dose 4) Initial concentration

4.5.1 Impact of Time

Contact time is essential in industrial applications since it allows us to obtain the quickest reaction time and most economical adsorption process. The influence of contact duration on the ability of beads to remove nitrate is being researched. In a 100ml mixture of 10 mg/L nitrate and 70 mg of iron oxide-encrusted chitosan beads at 24°C, the effect of contact time on nitrate adsorption was investigated. At 200 rpm, this assembly was agitated for two hours. The obtained data show that nitrate ion adsorption significantly increased over time. Adsorption occurs most quickly in the first 120 minutes. Adsorption will then reach its equilibrium level. This manner might result from functional groups being filled and a decrease in the number of accessible adsorption sites.

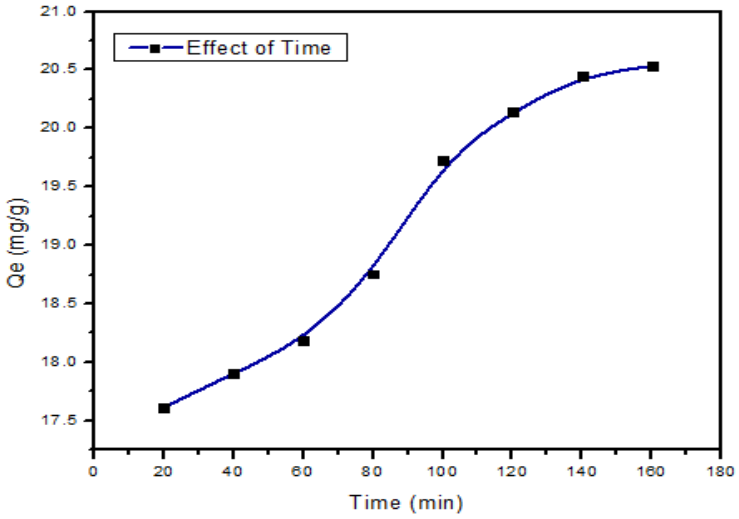

Figure 29: Graphical representation of the impact of time

4.5.2 Impact of pH

The impact of pH is a key factor in the adsorption system because it regulates the ionization behavior of the nitrate ions and the charge of the adsorbent surface. It is related to the reactive sites on the adsorbent surface's capacity for protonation and deprotonation of poisonous anions. This study looked at how the pH of the solution affected the removal of nitrate ions using iron oxide-encrusted chitosan beads. In this work, the adsorption of nitrate at various pH levels was calculated using 70 mg of beads and 100 ml of nitrate solution (3-9). The results of the pH effect showed that nitrate has a high adsorption effectiveness in the range of 4-6. The positive charge on the iron oxide-embedded chitosan beads' surface, which interacts electrostatically with negatively charged nitrate ions to achieve the desired results, can be linked to these results. As the pH of the solution increased from 7 to 9, the adsorption effectiveness dramatically declined. These results are explained by the electrostatic interaction between iron oxide-coated chitosan beads and negatively charged nitrate ions, which is induced by the competition of OH ions in the aqueous solution.

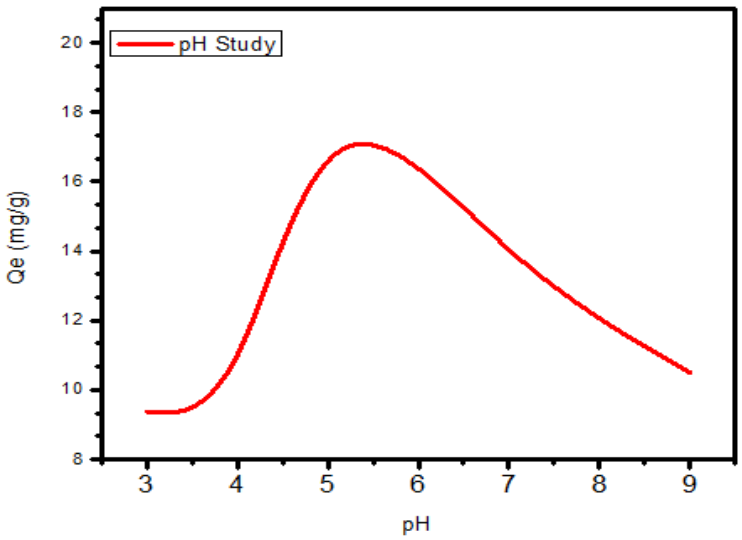

Figure 30: Graphical representation of the impact of pH

4.5.3 Impact of Dose

To evaluate the quantity of magnetic chitosan beads required for the effective and selective removal of nitrate from aqueous environments, several adsorbent dosage ranges (30-110mg) were used. It was observed that strategically increasing the dosage of magnetic chitosan beads improved the effectiveness of nitrate adsorption. The main cause of this occurrence is a rise in the dose of magnetic chitosan beads, which improves the reactive empty sites on the adsorbent surface and raises the adsorption effectiveness. The percentage of nitrate ions that are adsorbed also slightly increases when the adsorbent dosage is greater than 100 mg. The appropriate magnetic chitosan beads were fixed at 70 mg at the same time for additional adsorption study

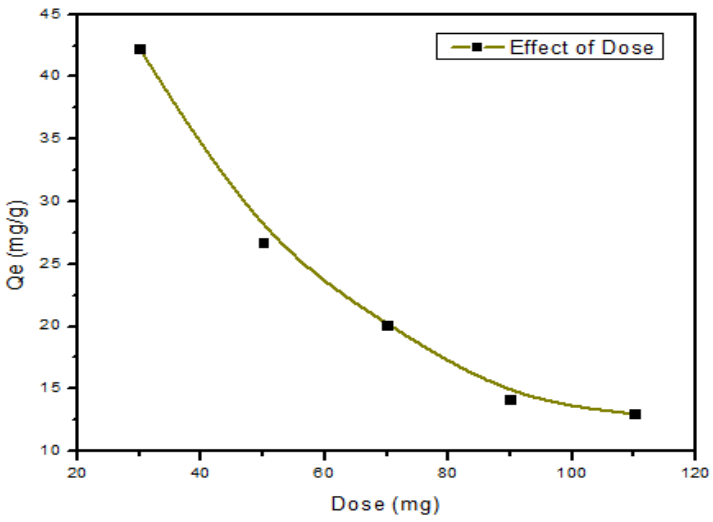

Figure 31: Graphical representation of the impact of dose

4.5.4 Impact of Initial Concentration

The batch process for the removal of nitrate from water was conducted to estimate the capability of hybrid beads. Using 70 mg of iron oxide-encrusted chitosan beads with 100 mL of nitrate mixture at pH of 5 for two hours, the effect of starting nitrate ion concentration upon the adsorption process was investigated at five different concentrations 10, 20, 30 40, and 50 mg/L. At first, the adsorption magnitude of chitosan beads increased sharply along with higher initial concentration of nitrate ions. The primary cause of this is because driving forces also increase due to larger concentration gradients at high nitrate ion concentrations. However, due to a reduction in the number of mobile adsorption sites, an equilibrium level of adsorption will be reached over time

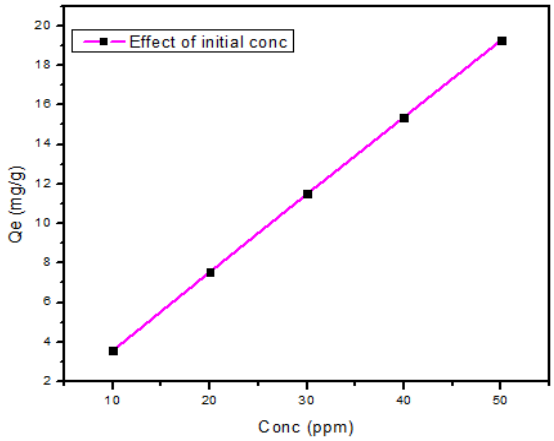

Figure 32: Graphical representation of the impact of initial concentration

4.6 Regeneration Experiment

Regenerating chitosan beads with iron oxide implants was the subject of several experiments. In a beaker containing 500 mg of a nitrate-containing solution (10 mg/L), the 200 mg sample was agitated for two hours at 24°C, 200 rpm, and 5 pH. The bead would then be thoroughly cleaned to remove the free Nitrate ions. The nitrate-filled beads will be stirred at 200 rpm with a temperature of 25 °C for 24 hours before being dipped in a 250 ml solution of 0.1 mol/L NaOH. The beads will then be rinsed in deionized water to reach a pH of neutral. After that, these beads were placed in a drying setup for 4 hours at 60 °C. These adsorption/desorption cycles were repeated until a noticeable decline in the performance of the beads occurred.

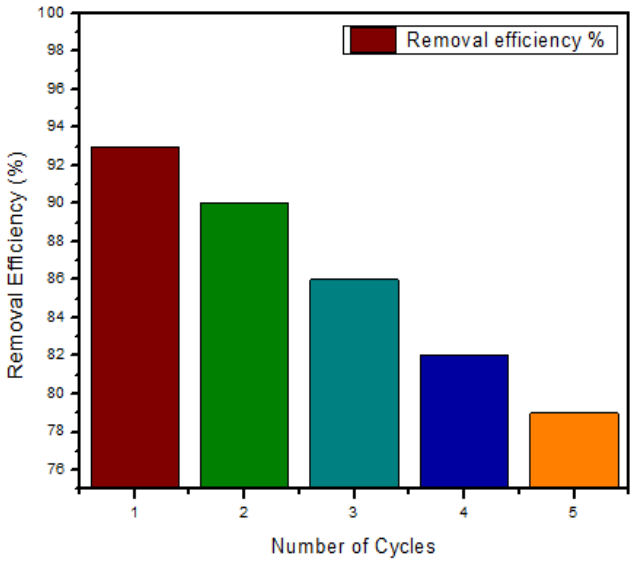

Figure 33: Graphical representation of regeneration cycles of iron oxide embedded chitosan beads

Conclusion

In this study nanoparticles of iron oxide prepared by the process of chemical co-precipitation were embedded in chitosan for the synthesis of beads. These beads were then used for the removal of nitrate ($N0_3^-$) ions from the mine wastewater by the process of adsorption. The characterizations of SEM, FTIR, XRD, BET and EDAX with mapping was analyzed for the surface and structural properties of the prepared beads. SEM analysis showed that the shape of beads was spherical and EDAX confirmed the presence of iron oxide and chitosan in the structure of the bead. Starting with the adsorption study the following two models were used for the analysis of batch testing results: Adsorption isotherm model and Adsorption kinetic model. The adsorption isotherm models resulted in the Langmuir value R^2 >0.99 and the Freundlich value R^2 > 0.98. The adsorption kinetic model resulted in the Kinetic First Order model value R^2> 0.89 and the Kinetic Second order model value R^2>0.99. Based on these results it was found that the isothermic study gave a homogeneous single layer adsorption by Langmuir isotherm model and the Pseudo second order kinetic model determined that chemisorption was the rate controlling step. Regeneration experiment was performed up to 5 cycles in which the efficiency of these beads for nitrate removal was dropped from 93% to 79%. Overall, this study demonstrated the efficient removal of nitrate ions from water.

Future Recommendation

For future recommendations,

- Different kinds of magnetic nanoparticles with chitosan for the synthesis of beads can be used and the removal efficiency of those beads can be noted, including the regeneration experiment up to several cycles.
- The beads used in this study can be used in industrial application for removal of different toxic ions present in water including but not limited nitrate ions.

References

[1] H. Liu, Z. Hu, Y. Zhang, J. Zhang, H. Xie, and S. Liang, "Microbial nitrogen removal of ammonia wastewater in poly (butylenes succinate)-based constructed wetland: effect of dissolved oxygen," (in eng), *Appl Microbiol Biotechnol,* vol. 102, no. 21, pp. 9389-9398, Nov 2018.

[2] Y. Chen, J. Hong, M. Tang, Y. Zheng, M. Qiu, and D. Ni, "Causal complexity of environmental pollution in China: a province-level fuzzy-set qualitative comparative analysis," (in eng), *Environ Sci Pollut Res Int,* Sep 28 2022.

[3] X. Hu, D. Sobotka, K. Czerwionka, Q. Zhou, L. Xie, and J. Makinia, "Effects of different external carbon sources and electron acceptors on interactions between denitrification and phosphorus removal in biological nutrient removal processes," (in eng), *J Zhejiang Univ Sci B,* vol. 19, no. 4, pp. 305-316, 2018 Apr. 2018.

[4] L. Li *et al.*, "Denitrification and microbial community in MBBR using A. donax as carbon source and biofilm carriers for reverse osmosis concentrate treatment," (in eng), *J Environ Sci (China),* vol. 84, pp. 133-143, Oct 2019.

[5] H. Astatkie, E. M. Beyene, and A. Ambelu, "Contamination and ecological risk assessment of toxic metals in Awetu watershed stream waters and sediments, Ethiopia," (in eng), *Environ Monit Assess,* vol. 194, no. 6, p. 451, May 24 2022.

[6] A. Moustafa, M. Hamzeh, M. Baroudi, B. Ouddane, and S. Net, "55 xenobiotic organic compounds in Tripoli landfill-Lebanon leachate and their fluxes to the Abou Ali River and Mediterranean Sea," (in eng), *Environ Monit Assess,* vol. 194, no. 12, p. 856, Oct 07 2022.

[7] B. Brindefalk *et al.*, "Bacterial composition in Swedish raw drinking water reveals three major interacting ubiquitous metacommunities," (in eng), *Microbiologyopen,* vol. 11, no. 5, p. e1320, Oct 2022.

[8] M. Rahimi, M. Zarei, B. Keshavarzi, R. Golshani, and S. G. G. Zafarani, "Water quality stress to Amirkalayeh Wetland, Northern Iran," (in eng), *Environ Monit Assess,* vol. 195, no. 1, p. 49, Oct 31 2022.

[9] R. Yuan, Z. Li, and S. Guo, "Health risks of shallow groundwater in the five basins of Shanxi, China: Geographical, geological and human activity roles," (in eng), *Environ Pollut,* p. 120524, Oct 26 2022.

[10] J. Qian, J. Zhou, Z. Zhang, R. Liu, and Q. Wang, "Biological Nitrogen Removal through Nitritation Coupled with Thiosulfate-Driven Denitritation," (in eng), *Sci Rep,* vol. 6, p. 27502, 06 08 2016.

[11] X. Chen, L. Zheng, M. Zhu, C. Jiang, X. Dong, and Y. Chen, "Quantitative identification of nitrate and sulfate sources of a multiple land-use area impacted by mine drainage," (in eng), *J Environ Manage,* vol. 325, no. Pt A, p. 116551, Oct 22 2022.

[12] E. Kelepertzis *et al.*, "Assessment of natural and anthropogenic contamination sources in a Mediterranean aquifer by combining hydrochemical and stable isotope techniques," (in eng), *Sci Total Environ,* p. 159763, Oct 26 2022.

[13] L. Zhang, Z. Xu, Y. Sun, Y. Gao, and L. Zhu, "Coal Mining Activities Driving the Changes in Microbial Community and Hydrochemical Characteristics of Underground Mine Water," (in eng), *Int J Environ Res Public Health,* vol. 19, no. 20, Oct 16 2022.

[14] S. Lv, Y. Zeng, L. Zhang, and H. Zhao, "Evaluation of coal seam floor water bursting in multi-aquifer Gequan coal mine, China," (in eng), *Sci Rep,* vol. 12, no. 1, p. 18076, Oct 27 2022.

[15] M. Pang, H. Pan, H. Zhang, and T. Zhang, "Experimental Investigation of the Effect of Groundwater on the Relative Permeability of Coal Bodies around Gas Extraction Boreholes," (in eng), *Int J Environ Res Public Health,* vol. 19, no. 20, Oct 20 2022.

[16] J. Y. A. Maréchal, K. Hendriksen, L. T. Hansen, C. Gundelund, and P. E. Jensen, "Domestic water supply in rural Greenland - sufficiency, affordability and

accessibility," (in eng), *Int J Circumpolar Health*, vol. 81, no. 1, p. 2138095, Dec 2022.
[17] Q. Chen, W. Wu, Y. Guo, J. Li, and F. Wei, "Environmental impact, treatment technology and monitoring system of ship domestic sewage: A review," (in eng), *Sci Total Environ*, vol. 811, p. 151410, Mar 10 2022.
[18] M. Zheng *et al.*, "Predictions of the Influent and Operational Conditions for Partial Nitritation with a Model Incorporating pH Dynamics," (in eng), *Environ Sci Technol*, vol. 52, no. 11, pp. 6457-6465, 06 05 2018.
[19] H. Liu, W. Zeng, M. He, C. Lin, W. Ouyang, and X. Liu, "Occurrence, distribution, and migration of antimony in the Zijiang River around a superlarge antimony deposit zone," (in eng), *Environ Pollut*, p. 120520, Oct 25 2022.
[20] S. E. Hale, M. S. Folde, U. H. Melby, E. U. Sjødahl, A. B. Smebye, and A. M. P. Oen, "From landfills to landscapes-Nature-based solutions for water management taking into account legacy contamination," (in eng), *Integr Environ Assess Manag*, vol. 18, no. 1, pp. 99-107, Jan 2022.
[21] Y. Gao, Y. W. Xie, Q. Zhang, A. L. Wang, Y. X. Yu, and L. Y. Yang, "Intensified nitrate and phosphorus removal in an electrolysis -integrated horizontal subsurface-flow constructed wetland," (in eng), *Water Res*, vol. 108, pp. 39-45, Jan 01 2017.
[22] D. E. Holmes, Y. Dang, and J. A. Smith, "Nitrogen cycling during wastewater treatment," (in eng), *Adv Appl Microbiol*, vol. 106, pp. 113-192, 2019.
[23] W. Wang, L. Cao, H. Tan, and R. Zhang, "Nitrogen removal from synthetic wastewater using single and mixed culture systems of denitrifying fungi, bacteria, and actinobacteria," (in eng), *Appl Microbiol Biotechnol*, vol. 100, no. 22, pp. 9699-9707, Nov 2016.
[24] H. Zhang *et al.*, "Nitrate removal characteristics and," (in eng), *Bioresour Technol*, vol. 307, p. 123230, Jul 2020.
[25] S. Singh *et al.*, "Nitrates in the environment: A critical review of their distribution, sensing techniques, ecological effects and remediation," (in eng), *Chemosphere*, vol. 287, no. Pt 1, p. 131996, Jan 2022.
[26] S. He, L. Ding, Y. Pan, H. Hu, L. Ye, and H. Ren, "Nitrogen loading effects on nitrification and denitrification with functional gene quantity/transcription analysis in biochar packed reactors at 5 °C," (in eng), *Sci Rep*, vol. 8, no. 1, p. 9844, 06 29 2018.
[27] Z. Wang *et al.*, "Enhanced adsorption and reduction performance of nitrate by Fe-Pd-Fe," (in eng), *Chemosphere*, vol. 281, p. 130718, Oct 2021.
[28] T. Reinhardt, A. N. Veizaga Campero, R. Minke, H. Schönberger, and E. Rott, "Batch Studies of Phosphonate and Phosphate Adsorption on Granular Ferric Hydroxide (GFH) with Membrane Concentrate and Its Synthetic Replicas," (in eng), *Molecules*, vol. 25, no. 21, Nov 09 2020.
[29] N. Lambert, P. Van Aken, R. Van den Broeck, and R. Dewil, "Adsorption of phosphate on iron-coated sand granules as a robust end-of-pipe purification strategy in the horticulture sector," (in eng), *Chemosphere*, vol. 267, p. 129276, Mar 2021.
[30] F. Ogata *et al.*, "Adsorption of Nitrite and Nitrate Ions from an Aqueous Solution by Fe-Mg-Type Hydrotalcites at Different Molar Ratios," (in eng), *Chem Pharm Bull (Tokyo)*, vol. 66, no. 4, pp. 458-465, 2018.
[31] G. Vilardi and L. Di Palma, "Kinetic Study of Nitrate Removal from Aqueous Solutions Using Copper-Coated Iron Nanoparticles," (in eng), *Bull Environ Contam Toxicol*, vol. 98, no. 3, pp. 359-365, Mar 2017.
[32] L. C. Santos, A. F. da Silva, P. V. Dos Santos Lins, J. L. da Silva Duarte, A. H. Ide, and L. Meili, "Mg-Fe layered double hydroxide with chloride intercalated: synthesis, characterization and application for efficient nitrate removal," (in eng), *Environ Sci Pollut Res Int*, vol. 27, no. 6, pp. 5890-5900, Feb 2020.
[33] Q. Hu, N. Chen, C. Feng, J. Zhang, W. Hu, and L. Lv, "Kinetic studies of nitrate removal from aqueous solution using granular chitosan-Fe(III) complex," (in eng), *Water Sci Technol*, vol. 73, no. 5, pp. 1211-20, 2016.

[34] B. Mehdinejadiani, S. M. Amininasab, and L. Manhooei, "Enhanced adsorption of nitrate from water by modified wheat straw: equilibrium, kinetic and thermodynamic studies," (in eng), *Water Sci Technol,* vol. 79, no. 2, pp. 302-313, Jan 2019.
[35] N. Amaly, A. Y. El-Moghazy, G. Sun, and P. Pandey, "Rapid removal of nitrate from liquid dairy manure by cationic poly (vinyl alcohol-co-ethylene) nanofiber membrane," (in eng), *J Environ Manage,* vol. 282, p. 111574, Mar 15 2021.
[36] T. Fundneider, V. Acevedo Alonso, A. Wick, D. Albrecht, and S. Lackner, "Implications of biological activated carbon filters for micropollutant removal in wastewater treatment," (in eng), *Water Res,* vol. 189, p. 116588, Feb 01 2021.
[37] T. Dong, "Nitrogen removal from groundwater using scoria: Kinetics, equilibria and microstructure," (in eng), *J Environ Sci Health A Tox Hazard Subst Environ Eng,* vol. 56, no. 4, pp. 386-393, 2021.
[38] H. Sun *et al.*, "Denitrification using excess activated sludge as carbon source: Performance and the microbial community dynamics," (in eng), *Bioresour Technol,* vol. 238, pp. 624-632, Aug 2017.
[39] H. A. T. Banu, P. Karthikeyan, S. Vigneshwaran, and S. Meenakshi, "Adsorptive performance of lanthanum encapsulated biopolymer chitosan-kaolin clay hybrid composite for the recovery of nitrate and phosphate from water," (in eng), *Int J Biol Macromol,* vol. 154, pp. 188-197, Jul 01 2020.
[40] S. Patra *et al.*, "Denitrification of nitrate in regeneration waste brine using hybrid cation exchanger supported nanoscale zero-valent iron with/without palladium nanoparticles," (in eng), *Chemosphere,* vol. 310, p. 136851, Oct 13 2022.
[41] B. Bishayee, R. P. Chatterjee, B. Ruj, S. Chakrabortty, and J. Nayak, "Strategic management of nitrate pollution from contaminated water using viable adsorbents: An economic assessment-based review with possible policy suggestions," (in eng), *J Environ Manage,* vol. 303, p. 114081, Feb 01 2022.
[42] A. Lejarazu-Larrañaga *et al.*, "Nitrate Removal by Donnan Dialysis and Anion-Exchange Membrane Bioreactor Using Upcycled End-of-Life Reverse Osmosis Membranes," (in eng), *Membranes (Basel),* vol. 12, no. 2, Jan 18 2022.
[43] D. Li, X. A. Ning, Y. Yuan, Y. Hong, and J. Zhang, "Ion-exchange polymers modified bacterial cellulose electrodes for the selective removal of nitrite ions from tail water of dyeing wastewater," (in eng), *J Environ Sci (China),* vol. 91, pp. 62-72, May 2020.
[44] L. Ding *et al.*, "Adsorptive removal of gallic acid from aqueous solution onto magnetic ion exchange resin," (in eng), *Water Sci Technol,* vol. 81, no. 7, pp. 1479-1493, Apr 2020.
[45] T. N. Dharmapriya, H. Y. Shih, and P. J. Huang, "Facile Synthesis of Hydrogel-Based Ion-Exchange Resins for Nitrite/Nitrate Removal and Studies of Adsorption Behavior," (in eng), *Polymers (Basel),* vol. 14, no. 7, Apr 01 2022.
[46] A. Bayrakdar, E. Tilahun, and B. Çalli, "Simultaneous nitrate and sulfide removal using a bio-electrochemical system," (in eng), *Bioelectrochemistry,* vol. 129, pp. 228-234, Oct 2019.
[47] W. Ye, W. Zhang, X. Hu, S. Yang, and W. Liang, "Efficient electrochemical-catalytic reduction of nitrate using Co/AC," (in eng), *Sci Total Environ,* vol. 732, p. 139245, Aug 25 2020.
[48] F. Yao *et al.*, "Indirect electrochemical reduction of nitrate in water using zero-valent titanium anode: Factors, kinetics, and mechanism," (in eng), *Water Res,* vol. 157, pp. 191-200, Jun 15 2019.
[49] M. Hong, Q. Wang, J. Sun, and C. Wu, "A highly active copper-nanoparticle-based nitrate reduction electrocatalyst prepared by in situ electrodeposition and annealing," (in eng), *Sci Total Environ,* vol. 827, p. 154349, Jun 25 2022.
[50] H. Olvera-Vargas, N. Oturan, C. T. Aravindakumar, M. M. Paul, V. K. Sharma, and M. A. Oturan, "Electro-oxidation of the dye azure B: kinetics, mechanism, and by-products," (in eng), *Environ Sci Pollut Res Int,* vol. 21, no. 14, pp. 8379-86, 2014.

[51] Z. Wu *et al.*, "Highly efficient nitrate removal in a heterotrophic denitrification system amended with redox-active biochar: A molecular and electrochemical mechanism," (in eng), *Bioresour Technol*, vol. 275, pp. 297-306, Mar 2019.
[52] A. Gafiullina, M. Mamelkina, P. Vehmaanperä, T. Kinnarinen, and A. Häkkinen, "Pressure filtration properties of sludge generated in the electrochemical treatment of mining waters," (in eng), *Water Res*, vol. 181, p. 115922, Aug 15 2020.
[53] K. S. Hashim, A. Shaw, R. Al Khaddar, M. O. Pedrola, and D. Phipps, "Energy efficient electrocoagulation using a new flow column reactor to remove nitrate from drinking water - Experimental, statistical, and economic approach," (in eng), *J Environ Manage*, vol. 196, pp. 224-233, Jul 01 2017.
[54] J. Lakshmi, G. Sozhan, and S. Vasudevan, "Recovery of hydrogen and removal of nitrate from water by electrocoagulation process," (in eng), *Environ Sci Pollut Res Int*, vol. 20, no. 4, pp. 2184-92, Apr 2013.
[55] D. Tibebe, A. Negash, M. Mulugeta, Y. Kassa, Z. Moges, and D. Yenealem, "Investigation of selected physico-chemical quality parameters in industrial wastewater by electrocoagulation process, Ethiopia," (in eng), *BMC Chem*, vol. 16, no. 1, p. 67, Sep 15 2022.
[56] C. Tsioptsias, D. Petridis, N. Athanasakis, I. Lemonidis, A. Deligiannis, and P. Samaras, "Post-treatment of molasses wastewater by electrocoagulation and process optimization through response surface analysis," (in eng), *J Environ Manage*, vol. 164, pp. 104-13, Dec 01 2015.
[57] F. Özyonar and M. U. Korkmaz, "Sequential use of the electrocoagulation-electrooxidation processes for domestic wastewater treatment," (in eng), *Chemosphere*, vol. 290, p. 133172, Mar 2022.
[58] M. Zhu *et al.*, "Current intensities altered the performance and microbial community structure of a bio-electrochemical system," (in eng), *Chemosphere*, vol. 265, p. 129069, Feb 2021.
[59] A. Atrashkevich, A. S. Fajardo, P. Westerhoff, W. S. Walker, C. M. Sánchez-Sánchez, and S. Garcia-Segura, "Overcoming barriers for nitrate electrochemical reduction: By-passing water hardness," (in eng), *Water Res*, vol. 225, p. 119118, Oct 15 2022.
[60] S. Jia, Y. Han, H. Zhuang, H. Han, and K. Li, "Simultaneous removal of organic matter and salt ions from coal gasification wastewater RO concentrate and microorganisms succession in a MBR," (in eng), *Bioresour Technol*, vol. 241, pp. 517-524, Oct 2017.
[61] E. Li, R. Wang, X. Jin, S. Lu, Z. Qiu, and X. Zhang, "Investigation into the nitrate removal efficiency and microbial communities in a sequencing batch reactor treating reverse osmosis concentrate produced by a coking wastewater treatment plant," (in eng), *Environ Technol*, vol. 39, no. 17, pp. 2203-2214, Sep 2018.
[62] A. Lejarazu-Larrañaga, J. M. Ortiz, S. Molina, Y. Zhao, and E. García-Calvo, "Nitrate-Selective Anion Exchange Membranes Prepared using Discarded Reverse Osmosis Membranes as Support," (in eng), *Membranes (Basel)*, vol. 10, no. 12, Nov 27 2020.
[63] C. P. Leo, M. Z. Yahya, S. N. Kamal, A. L. Ahmad, and A. W. Mohammad, "Potential of nanofiltration and low pressure reverse osmosis in the removal of phosphorus for aquaculture," (in eng), *Water Sci Technol*, vol. 67, no. 4, pp. 831-7, 2013.
[64] V. Nagaraj, L. Skillman, G. Ho, D. Li, and A. Gofton, "Characterisation and comparison of bacterial communities on reverse osmosis membranes of a full-scale desalination plant by bacterial 16S rRNA gene metabarcoding," (in eng), *NPJ Biofilms Microbiomes*, vol. 3, p. 13, 2017.
[65] M. Simonič, "Reverse Osmosis Treatment of Wastewater for Reuse as Process Water-A Case Study," (in eng), *Membranes (Basel)*, vol. 11, no. 12, Dec 10 2021.
[66] Z. Li *et al.*, "Synthesis and characterization of a surface-grafted Pb(ii)-imprinted polymer based on activated carbon for selective separation and pre-concentration of Pb(ii) ions from environmental water samples," (in eng), *RSC Adv*, vol. 9, no. 9, pp. 5110-5120, Feb 05 2019.

[67] L. Yang *et al.*, "Functionalized Ultrasmall Iron Oxide Nanoparticles for," (in eng), *Molecules*, vol. 27, no. 20, Oct 15 2022.
[68] A. D. Wulandari, S. Sutriyo, and R. Rahmasari, "Synthesis conditions and characterization of superparamagnetic iron oxide nanoparticles with oleic acid stabilizer," (in eng), *J Adv Pharm Technol Res*, vol. 13, no. 2, pp. 89-94, 2022 Apr-Jun 2022.
[69] Y. Liu, L. Meng, K. Han, and S. Sun, "Synthesis of nano-zirconium-iron oxide supported by activated carbon composite for the removal of Sb(v) in aqueous solution," (in eng), *RSC Adv*, vol. 11, no. 49, pp. 31131-31141, Sep 14 2021.
[70] S. H. Luo, D. B. Hu, H. Liu, J. Z. Li, and T. F. Yi, "Hydrothermal synthesis and characterization of α-Fe," (in eng), *J Hazard Mater*, vol. 368, pp. 714-721, Apr 15 2019.
[71] B. T. Hang, T. T. Anh, and D. H. Thang, "Hydrothermal Synthesis of," (in eng), *J Nanosci Nanotechnol*, vol. 21, no. 4, pp. 2545-2551, 04 01 2021.
[72] Z. Ignatovich *et al.*, "One-Step Synthesis of Magnetic Nanocomposite with Embedded Biologically Active Substance," (in eng), *Molecules*, vol. 26, no. 4, Feb 10 2021.
[73] N. Yadav, A. Singh, and M. Kaushik, "Hydrothermal synthesis and characterization of magnetic Fe," (in eng), *J Mater Sci Mater Med*, vol. 31, no. 8, p. 68, Jul 23 2020.
[74] H. Wang, P. Shi, and J. Ning, "Synthesis, Characterization, and Electrochemical Properties of La-Doped α-Fe," (in eng), *Nanomaterials (Basel)*, vol. 12, no. 19, Sep 26 2022.
[75] C. D. Park, J. Walker, R. Tannenbaum, A. E. Stiegman, J. Frydrych, and L. Machala, "Sol-gel-derived iron oxide thin films on silicon: surface properties and interfacial chemistry," (in eng), *ACS Appl Mater Interfaces*, vol. 1, no. 9, pp. 1843-6, Sep 2009.
[76] A. Taufik and R. Saleh, "Synthesis of iron(II,III) oxide/zinc oxide/copper(II) oxide (Fe," (in eng), *J Colloid Interface Sci*, vol. 491, pp. 27-36, Apr 01 2017.
[77] S. Laurent, J. L. Bridot, L. V. Elst, and R. N. Muller, "Magnetic iron oxide nanoparticles for biomedical applications," (in eng), *Future Med Chem*, vol. 2, no. 3, pp. 427-49, Mar 2010.
[78] A. Hussain, A. P. Jadhav, Y. K. Baek, H. J. Choi, J. Lee, and Y. S. Kang, "One pot synthesis of exchange coupled Nd2Fe14B/alpha-Fe by pechini type sol-gel method," (in eng), *J Nanosci Nanotechnol*, vol. 13, no. 11, pp. 7717-22, Nov 2013.
[79] A. Darmawan, S. Smart, A. Julbe, and J. C. Diniz da Costa, "Iron Oxide Silica Derived from Sol-Gel Synthesis," (in eng), *Materials (Basel)*, vol. 4, no. 2, pp. 448-456, Feb 17 2011.
[80] S. Ayyanaar *et al.*, "ROS-Responsive Chitosan Coated Magnetic Iron Oxide Nanoparticles as Potential Vehicles for Targeted Drug Delivery in Cancer Therapy," (in eng), *Int J Nanomedicine*, vol. 15, pp. 3333-3346, 2020.
[81] Q. Chang, A. Ali, J. Su, Q. Wen, Y. Bai, and Z. Gao, "Simultaneous removal of nitrate, manganese, and tetracycline by Zoogloea sp. MFQ7: Adsorption mechanism of tetracycline by biological precipitation," (in eng), *Bioresour Technol*, vol. 340, p. 125690, Nov 2021.
[82] L. Lv *et al.*, "Progress in Iron Oxides Based Nanostructures for Applications in Energy Storage," (in eng), *Nanoscale Res Lett*, vol. 16, no. 1, p. 138, Aug 31 2021.
[83] A. Lassenberger *et al.*, "Monodisperse Iron Oxide Nanoparticles by Thermal Decomposition: Elucidating Particle Formation by Second-Resolved in Situ Small-Angle X-ray Scattering," (in eng), *Chem Mater*, vol. 29, no. 10, pp. 4511-4522, May 23 2017.
[84] M. Unni *et al.*, "Thermal Decomposition Synthesis of Iron Oxide Nanoparticles with Diminished Magnetic Dead Layer by Controlled Addition of Oxygen," (in eng), *ACS Nano*, vol. 11, no. 2, pp. 2284-2303, 02 28 2017.
[85] A. Maier *et al.*, "From Structure to Function: Understanding Synthetic Conditions in Relation to Magnetic Properties of Hybrid Pd/Fe-Oxide Nanoparticles," (in eng), *Nanomaterials (Basel)*, vol. 12, no. 20, Oct 18 2022.

[86] Q. Zeng, I. Baker, J. A. Loudis, Y. F. Liao, and P. J. Hoopes, "Synthesis and heating effect of iron/iron oxide composite and iron oxide nanoparticles," (in eng), *Proc SPIE Int Soc Opt Eng,* vol. 6440, p. 64400H, Feb 09 2007.
[87] K. Drønen *et al.*, "Modeling of heavy nitrate corrosion in anaerobe aquifer injection water biofilm: a case study in a flow rig," (in eng), *Environ Sci Technol,* vol. 48, no. 15, pp. 8627-35, 2014.
[88] S. A. Elsuccary and A. A. Salem, "Novel flow injection analysis methods for the determination of total iron in blood serum and water," (in eng), *Talanta,* vol. 131, pp. 108-15, Jan 2015.
[89] R. Hachani *et al.*, "Correction: Polyol synthesis, functionalisation, and biocompatibility studies of superparamagnetic iron oxide nanoparticles as potential MRI contrast agents," (in eng), *Nanoscale,* vol. 8, no. 7, p. 4395, Feb 21 2016.
[90] D. Leybo *et al.*, "Ascorbic Acid-Assisted Polyol Synthesis of Iron and Fe/GO, Fe/h-BN Composites for Pb," (in eng), *Nanomaterials (Basel),* vol. 10, no. 1, Dec 22 2019.
[91] H. Moradpoor *et al.*, "An overview of recent progress in dental applications of zinc oxide nanoparticles," (in eng), *RSC Adv,* vol. 11, no. 34, pp. 21189-21206, Jun 09 2021.
[92] P. Karthikeyan and S. Meenakshi, "Fabrication of hybrid chitosan encapsulated magnetic-kaolin beads for adsorption of phosphate and nitrate ions from aqueous solutions," (in eng), *Int J Biol Macromol,* vol. 168, pp. 750-759, Jan 31 2021.
[93] M. P. Kesavan *et al.*, "Magnetic iron oxide nanoparticles (MIONs) cross-linked natural polymer-based hybrid gel beads: Controlled nano anti-TB drug delivery application," (in eng), *J Biomed Mater Res A,* vol. 106, no. 4, pp. 1039-1050, Apr 2018.
[94] J. Wu, X. Cheng, Y. Li, and G. Yang, "Constructing biodegradable nanochitin-contained chitosan hydrogel beads for fast and efficient removal of Cu(II) from aqueous solution," (in eng), *Carbohydr Polym,* vol. 211, pp. 152-160, May 01 2019.
[95] Y. Wang, J. Su, A. Ali, Q. Chang, Y. Bai, and Z. Gao, "Enhanced nitrate, manganese, and phenol removal by polyvinyl alcohol/sodium alginate with biochar gel beads immobilized bioreactor: Performance, mechanism, and bacterial diversity," (in eng), *Bioresour Technol,* vol. 348, p. 126818, Mar 2022.
[96] S. Chatterjee and S. H. Woo, "The removal of nitrate from aqueous solutions by chitosan hydrogel beads," (in eng), *J Hazard Mater,* vol. 164, no. 2-3, pp. 1012-8, May 30 2009.
[97] T. Baran, "Pd NPs@Fe," (in eng), *Carbohydr Polym,* vol. 237, p. 116105, Jun 01 2020.
[98] S. V. Durán, B. Lapo, M. Meneses, and A. M. Sastre, "Recovery of Neodymium (III) from Aqueous Phase by Chitosan-Manganese-Ferrite Magnetic Beads," (in eng), *Nanomaterials (Basel),* vol. 10, no. 6, Jun 19 2020.
[99] X. Song, G. Yan, S. Quan, E. Jin, J. Quan, and G. Jin, "MRI-visible liposome-polyethylenimine complexes for DNA delivery: preparation and evaluation," (in eng), *Biosci Biotechnol Biochem,* vol. 83, no. 4, pp. 622-632, Apr 2019.
[100] G. Lujanienė *et al.*, "Preparation of Graphene Oxide-Maghemite-Chitosan Composites for the Adsorption of Europium Ions from Aqueous Solutions," (in eng), *Molecules,* vol. 27, no. 22, Nov 19 2022.
[101] A. Sowmya and S. Meenakshi, "A novel quaternized chitosan-melamine-glutaraldehyde resin for the removal of nitrate and phosphate anions," (in eng), *Int J Biol Macromol,* vol. 64, pp. 224-32, Mar 2014.
[102] P. A. Jeshvaghani, M. Pourmadadi, F. Yazdian, H. Rashedi, K. Khoshmaram, and M. N. Nigjeh, "Synthesis and characterization of a novel, pH-responsive sustained release nanocarrier using polyethylene glycol, graphene oxide, and natural silk fibroin protein by a green nano emulsification method to enhance cancer treatment," (in eng), *Int J Biol Macromol,* Nov 23 2022.
[103] M. Kula-Maximenko, K. J. Zieliński, J. Depciuch, J. Lekki, M. Niemiec, and I. Ślesak, "Application of Spectroscopic Methods for the Identification of Superoxide Dismutases in Cyanobacteria," (in eng), *Int J Mol Sci,* vol. 23, no. 22, Nov 10 2022.

[104] S. Wang, H. Zhu, and Q. Meng, "Preparation and Characterization of Nanofibrous Membranes Electro-Spun from Blended Poly(l-lactide-co-ε-caprolactone) and Recombinant Spider Silk Protein as Potential Skin Regeneration Scaffold," (in eng), *Int J Mol Sci*, vol. 23, no. 22, Nov 14 2022.
[105] S. Saqib *et al.*, "Synthesis, characterization and use of iron oxide nano particles for antibacterial activity," (in eng), *Microsc Res Tech*, vol. 82, no. 4, pp. 415-420, Apr 2019.